AD-A033 196 PRATT AND WHITNEY AIRCRAFT EAST HARTFORD CONN F/G 21/5
ADVANCED CERAMIC TURBINE SEAL SYSTEM, PHASES II AND III.(U)
NOV 76 N00140-74-C-0586
UNCLASSIFIED PWA-5426 NL

1 OF 1
ADA033196

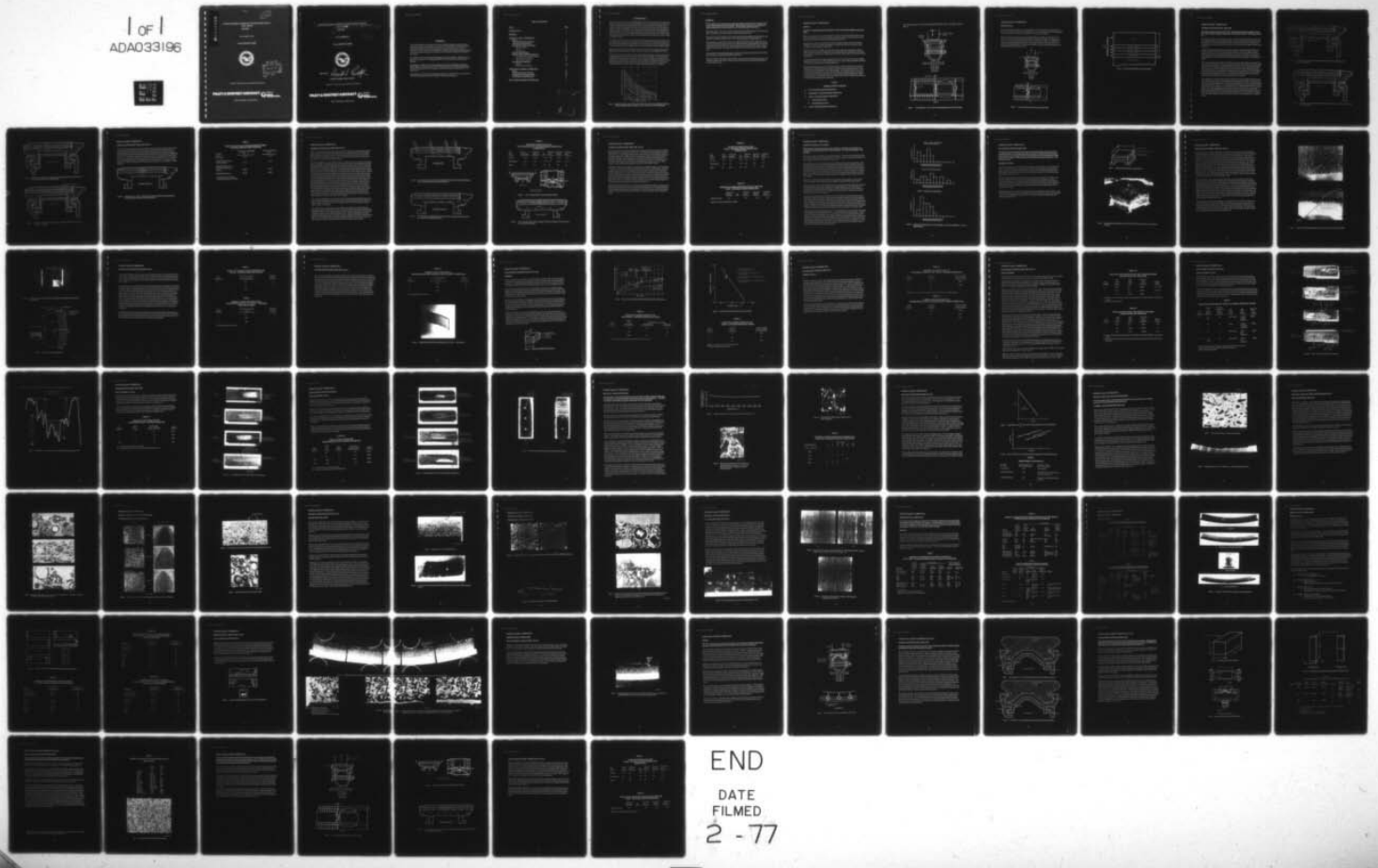

END

DATE
FILMED
2 -77

ADVANCED CERAMIC TURBINE SEAL SYSTEM, PHASES II AND III

FINAL REPORT

PWA-5426

29 NOVEMBER 1976

Contract N00140-74-C-0586

PRATT & WHITNEY AIRCRAFT Division of UNITED TECHNOLOGIES™

EAST HARTFORD, CONNECTICUT

(6) ADVANCED CERAMIC TURBINE SEAL SYSTEM, PHASES II AND III.

(9) FINAL REPORT. 1 Mar 74-15 Jun 76.

PWA-5426

(14)

(11) 29 NOVEMBER 1976

(12) 88 p.

Contract N00140-74-C-0586

(15)

Approved by: Donald S. Rudolph

Donald S. Rudolph, Program Director

APPROVAL FOR PUBLIC RELEASE; DISTRIBUTION UNLIMITED.

PRATT & WHITNEY AIRCRAFT Division of UNITED TECHNOLOGIES™

EAST HARTFORD, CONNECTICUT

287 500

FOREWORD

This document presents a summary of the work conducted during the complete contract period from 1 March 1974 through 15 June 1976 by Pratt & Whitney Aircraft Division of United Technologies Corporation, East Hartford, Connecticut under Navy Contract N00140-74-C-0586. The report is submitted in compliance with Sequence Number A003 of the Contract Data Requirements List, DD Form 1423, Exhibit A (Schedule Item 0003) of the contract.

Mr. Joseph W. Glatz of the Naval Air Propulsion Test Center (NAPTC), 1440 Parkway Avenue (PE43), Trenton, N. J., Telephone (609) 882-1414, Extension 224, was the Project Manager.

Mr. Matthew J. Wallace was the Program Manager for United Technologies Corporation, Pratt & Whitney Aircraft Group, Government Products Division, West Palm Beach, Florida (E40), from the inception of the program. His telephone number is (305) 844-3711, Extension 3237.

Appreciation is extended for overall program assistance to Pratt & Whitney Aircraft personnel Gerald A. Majocha and Robert H. Weidner, Experimental Engineers.

TABLE OF CONTENTS

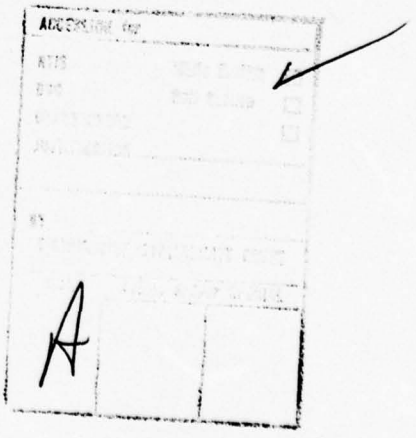

INTRODUCTION

The turbine outer air seal effort at Pratt & Whitney Aircraft has shown that seal surface temperature is most frequently the life limiting parameter. The present turbine seal systems for advanced engines utilize metal seals with advanced cooling techniques to maintain the required seal surface temperatures. Ceramic seal systems offer the potential of operating at a higher seal surface temperature which reduces the cooling requirements and complexity of cooling techniques. A guideline for cooling flow requirements at various material temperatures is shown in Figure 1. The figure indicates that advanced engines would experience significant reductions in required cooling if the allowable material temperature could be raised to 2600°F or higher.

The objective of the Advanced Ceramic Turbine Seal System Program is the design of a ceramic turbine blade outer air seal compatible with the Contractor's ATEGG spool which utilizes the Navy PCT (High Pressure Turbine). The program objective will provide technology to complement the Navy PCT (High Pressure Turbine) program and planned ATEGG effort.

The present Advanced Ceramic Turbine Seal System Program is a two-phase (Phases II and III) follow-on effort to the Phase I effort carried out under contract N00140-73-C-0320.

Phase II of the program consisted of rig specimen design, fabrication, testing and data analysis utilizing two ceramic systems selected at the completion of Phase I. These results provided the basis for a joint selection of one ceramic system for additional evaluation, and an initial engine ceramic turbine seal design resulted from Phase II. Phase III provides for a continual improvement of design, fabrication, and testing which culminates in a final engine ceramic turbine outer air seal design, compatible with the PCT turbine and ATEGG.

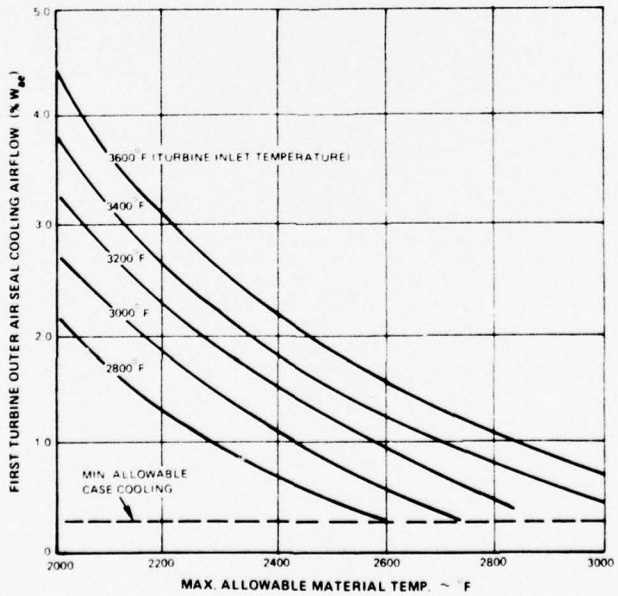

Figure 1 Required Cooling Air Flow (% Wae) for Convection Cooled First Turbine Blade Tip Seal Versus Maximum Allowable Material Temperature (°F) for Various Turbine Inlet Temperatures

SUMMARY

"Final" design of the advanced engine graded ZrO_2-NiCr turbine seal which includes thermal and structural analysis has been completed. Thermal fatigue, erosion and rub tolerance rig testing exceeded performance requirements with improved quality ceramic seals.

Mechanical design of the "final" advanced engine graded ZrO_2-NiCr turbine seal has been completed. This design is compatible with an advanced engine seal design.

Thermal and structural analysis of the "final" advanced engine graded ZrO_2-NiCr turbine seal predicted acceptable temperature and stress levels utilizing $\approx 0.75\%$ $W_{(ae)}$ cooling air.

Thermal fatigue, erosion and rub tests of the graded ZrO_2-NiCr advanced engine turbine seal with improved quality ceramic seals have exceeded performance requirements with a thermal fatigue life greater than 500 cycles, erosion life greater than 1600 hours for 10 mils ceramic erosion and rub tolerance which produces 10 mils of ceramic wear with less than 1 mil blade wear.

X-ray inspection and superficial hardness are effective non-destructive techniques for controlling the quality of the graded ZrO_2-NiCr turbine seal.

Structural ceramic (SiC) turbine seal exhibited extremely poor rub tolerance and posed a very difficult compliant attachment problem to prevent high stresses (point loading) throughout the total engine cycle.

GRADED ZrO_2-NiCr TURBINE SEAL

DESIGN

The "final" advanced engine graded ZrO_2-NiCr turbine seal mechanical design has been completed.

Major considerations of the graded ZrO_2-NiCr turbine seal mechanical design, which is compatible with a P&WA advanced engine design, involved the graded ceramic-to-metal concept, effective cooling schemes, and minimum leakage requirements.

Impingement cooling was selected for its design flexibility and high cooling effectiveness. Flexibility to tailor the cooling by adjusting the impingement hole size, spacing and standoff distance was a significant consideration.

Minimum leakage both radially and axially was another important consideration. Radial leakage refers to the loss of cooling air into the main gaspath, and axial leakage refers to the main gaspath air that bypasses turbine blades and flows between graded ceramic-metal turbine seal segments.

The graded ZrO_2-NiCr seal system progressed from the "first" design through several design iterations (Table I) to be the "first modification" of the "initial" design essentially unchanged except for layer thickness and cooling configuration.

With the high allowable ZrO_2 seal surface temperatures (2600°F and higher), and effective impingement cooling, the predicted cooling air would be reduced approximately 2.7% W_{ae} as compared to a transpiration cooled all-metal design. The axial gap, shown in View A of Figure 1, was determined to be in the range of 0.007 mils, requiring design of an axial step at the butt ends of the segments (Figure 1) to interrupt the straight through path. Design of radial seals for the graded ZrO_2-NiCr seal design is identical to the concept used previously for the all-metal advanced engine seal design.

TABLE I

NOMENCLATURE OF DESIGNS

- "FIRST" ADVANCED ENGINE TURBINE SEAL
- "PRELIMINARY" ADVANCED ENGINE TURBINE SEAL
- "INITIAL" ADVANCED ENGINE TURBINE SEAL
  - "FIRST MODIFICATION"
  - "SECOND MODIFICATION"
- "FINAL" ADVANCED ENGINE TURBINE SEAL

The "first modification" advanced engine graded ZrO_2-NiCr turbine seal design is shown in Figure 1.

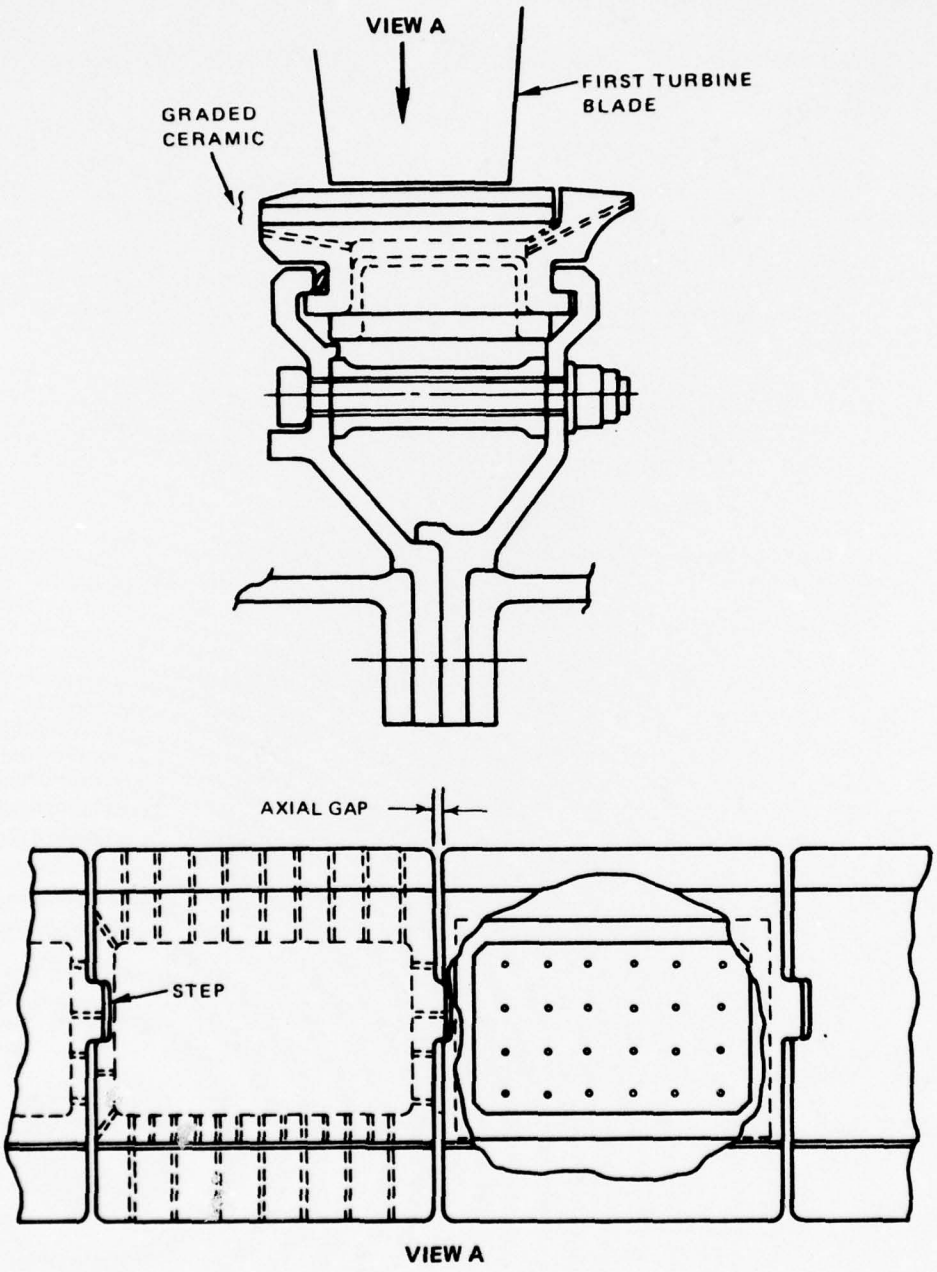

Figure 1 "First Modification" of the "Initial" Advanced Engine Ceramic Turbine Seal Design

GRADED ZrO_2-NiCr TURBINE SEAL

DESIGN (Cont'd)

Work was initiated during the "second modification" to design a graded ceramic-metal seal system that reduces the number of segments from 32 to 6. In addition, the metal trailing edge was removed and the ceramic layer extended over the entire I.D. surface.

The "final" advanced engine ceramic seal design (Figure 2) is made up of six 60° arc seal segments, each of which is fabricated by welding 3 component 20 degree arc segments together. This design further reduced performance penalties to the engine by minimizing the cooling air and main gas path leakage area. The graded ZrO_2-NiCr seal system utilized in this design is shown in Figure 3. It depicts the number of layers, thickness dimensions, and relative graded ZrO_2-NiCr percentages.

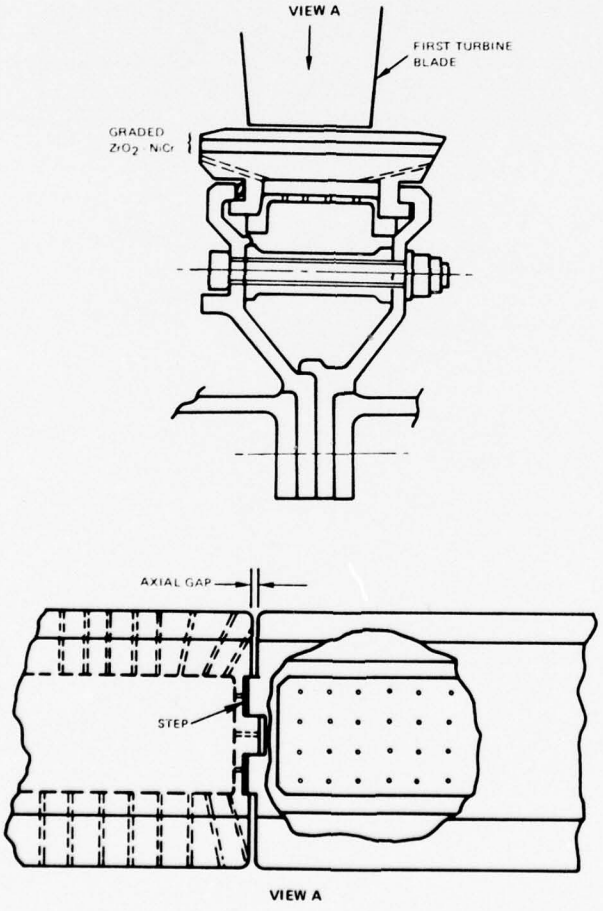

Figure 2 "Final" Advanced Engine Ceramic Turbine Seal Design

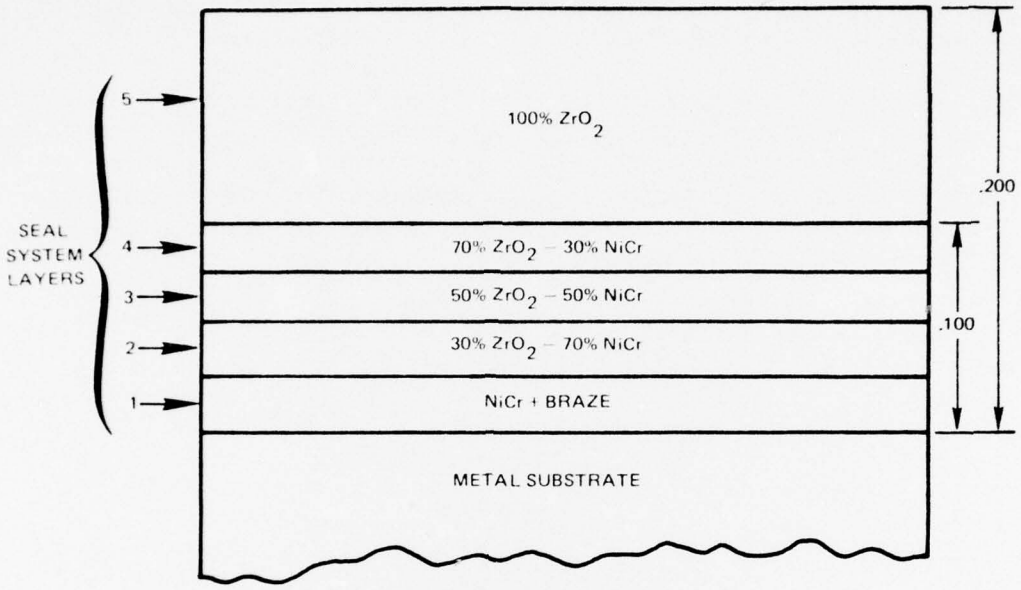

Figure 3 Graded Ceramic/Metal Material Seal System Design

GRADED ZrO_2-NiCr TURBINE SEAL

THERMAL AND STRUCTURAL ANALYSIS

Thermal and structural analysis of the "final" advanced engine graded ZrO_2-NiCr turbine seal system indicates acceptable temperature and stress levels utilizing $\approx$ 0.75% W_{ae} cooling air.

Throughout Phase II a thermal analysis, using a two-dimensional finite-difference heat transfer computer program, was conducted through a complete engine start up, acceleration and deceleration cycle between idle and full power. Also a structural analysis utilizing a two-dimensional finite-element computer program for the maximum stress engine conditions was performed.

A factor of major concern that was considered throughout Phase II and Phase III was the thermal distortion of the seal. Since all design iterations contain a low elastic modulus ceramic surface layer of the graded ZrO_2-NiCr seal and low thermal gradient through the metal segment the radial distortion during engine operation is predicted to be less than 4 mils compared to the 0.015 inch for the first generation advanced engine metal turbine seal design.

The "first" advanced engine graded ZrO_2-NiCr turbine seal design utilized a conservative design criteria that required 1.5% W_{ae} cooling air less than the first generation advanced engine metal turbine seal design to meet design temperature limits. Figure 1 displays the thermal map for the worst condition (full power hot spot) and Figure 2 shows the associated predicted thermal stresses. The compressive stresses shown are all within the allowable limit except for the top 50 mils of ZrO_2 layer. Creep relaxation and plastic flow of the top 0.050 inches of ZrO_2 was predicted to occur and thermal tests produced mud-flat type surface cracks which were stable and did not cause failure of the specimens.

The "preliminary" advanced engine graded ZrO_2-NiCr turbine seal design utilized the then current design system criteria to determine gas path temperature conditions with predicted lower hot spot temperatures than the previously used design criteria. The cooling air requirement was able to be reduced to $< 1.0\%$ W_{ae} and still meet design temperature limits for the full power hot spot condition in the "as fabricated" and "20 mil rubbed" (Figure 3) configurations. Structural analyses predicted that the stress levels did not exceed the strength limits of the graded ZrO_2-NiCr seal except for the predicted mud-flat cracking for the full power hot spot condition of the "as fabricated" (Figure 4) and "20 mil rubbed" configurations. Mud-flat cracking to a depth of about 0.035 inches was predicted but is considered stable.

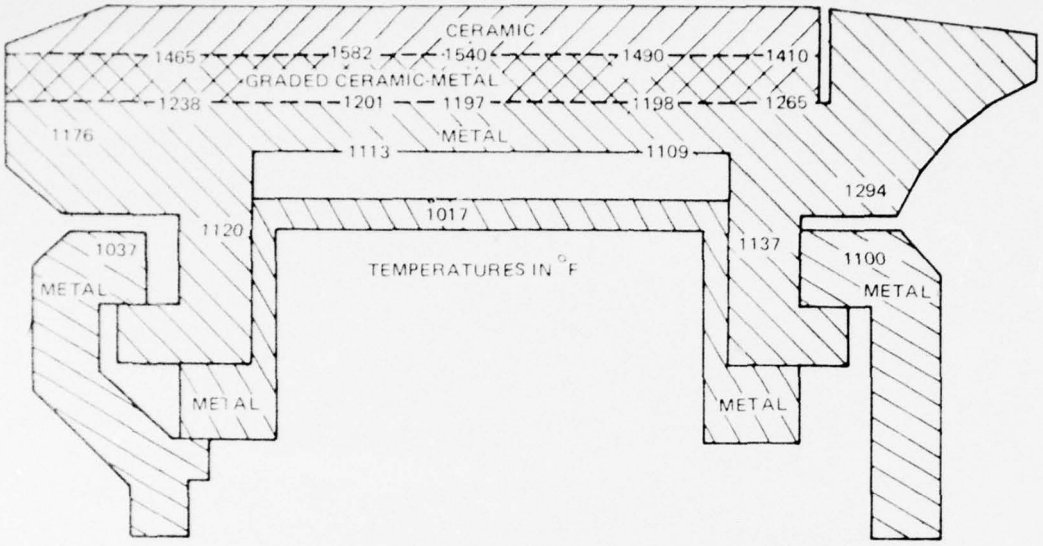

Figure 1 Thermal Map of "First" Advanced Engine Graded ZrO_2-NiCr Turbine Seal Design for Full Power Hot Spot Conditions

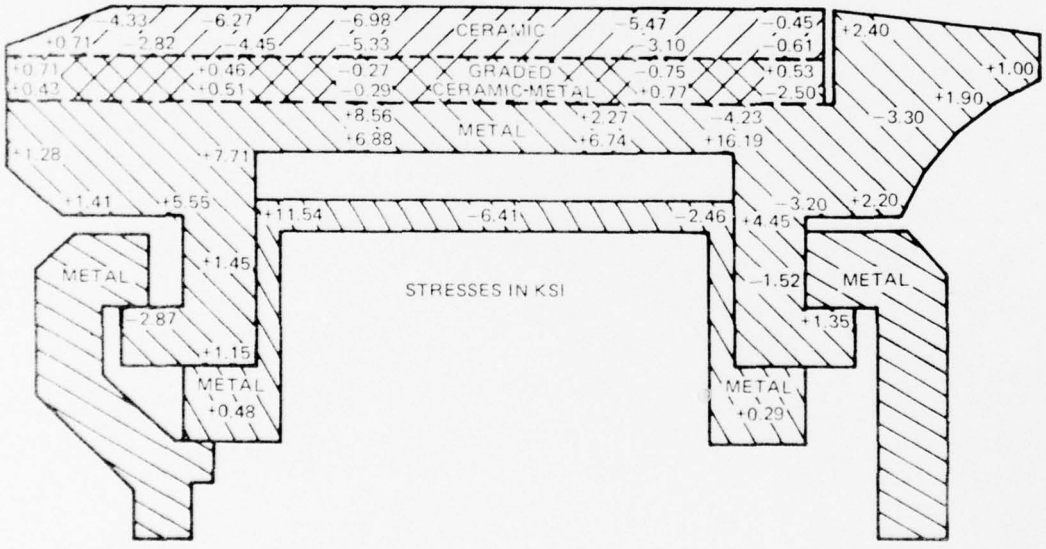

Figure 2 Stress Map of "First" Advanced Engine Graded ZrO_2-NiCr Turbine Seal Design for Full Power Hot Spot Conditions

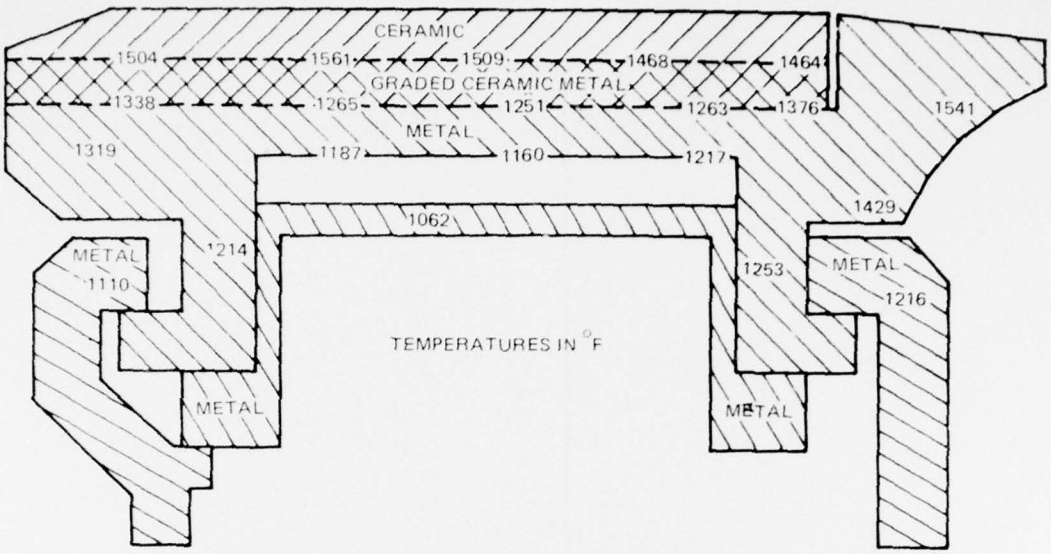

Figure 3 Thermal Map of "Preliminary" Advanced Engine Graded ZrO_2-NiCr Turbine Seal Design for Full Power Hot Spot Conditions "Rubbed 20 Mils"

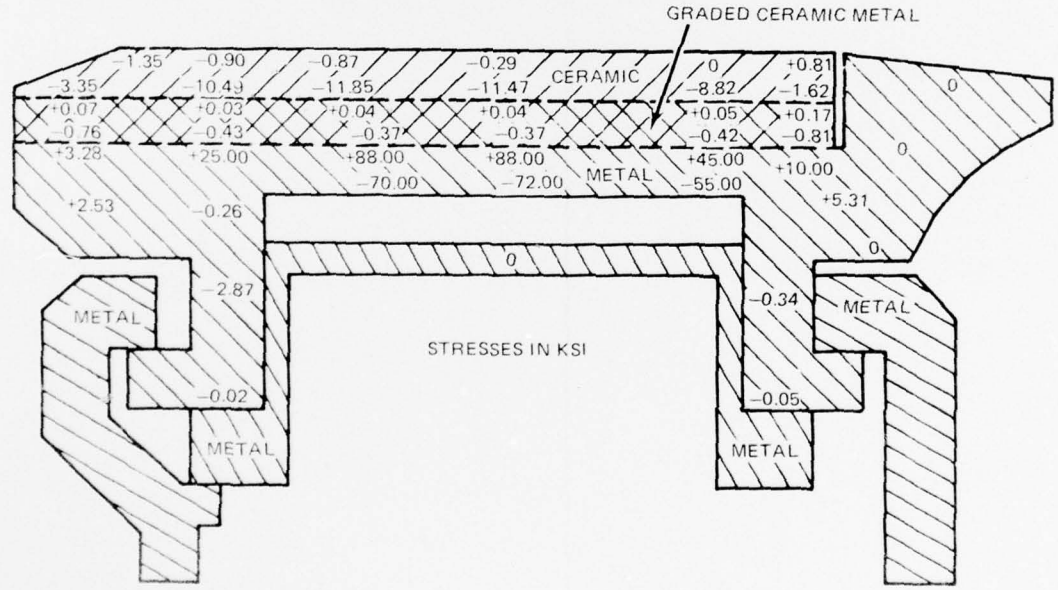

Figure 4 Map of the "As-Fabricated "Prestresses in the "Preliminary" Advanced Engine Graded ZrO_2-NiCr Turbine Seal

GRADED ZrO_2-NiCr TURBINE SEAL

THERMAL & STRUCTURAL ANALYSIS (Cont'd)

The "initial" advanced engine graded ZrO_2-NiCr turbine seal design utilized the same design criteria as for the "preliminary" design with newly measured physical properties of the graded ZrO_2-NiCr seal and a more uniform detailed element break-up of the thermal and structural two-dimensional finite-element analysis particularly at the leading and trailing edge locations. To maintain acceptable thermal levels the cooling air requirement remained the same as the "preliminary" design for the full power hot spot condition in the "as fabricated" and "20 mil rubbed" (Figure 5) configurations. Structural analysis of the "initial" design predicts an overall general reduction in stress levels as compared to the "preliminary" design (Table I).

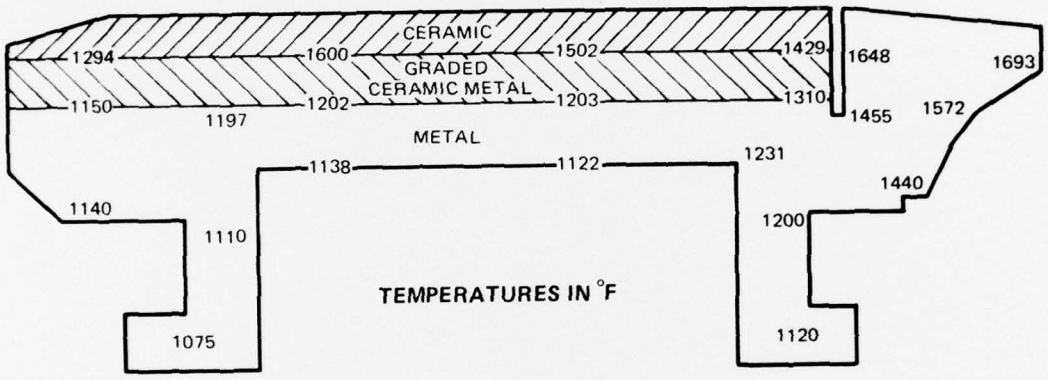

Figure 5 **Thermal Map of the "Initial" Advanced Engine Graded ZrO_2-NiCr Turbine Seal Design for Full Power Hot Spot Condition After an .020 Inch Rub**

TABLE I

GRADED ZrO_2-NiCr SEAL SYSTEM MAXIMUM STRESSES* FOR FULL POWER HOT SPOT CONDITION

Location	"Preliminary" Seal Design (ksi)	"Initial" Seal Design (ksi)
ZrO_2 Layer	−5.18	−3.73
Graded ZrO_2-NiCr Layer at ZrO_2 Interface	−0.21	−0.11
MAR-M-509 Substrate at Graded ZrO_2-NiCr Layer Interface	+40.00	+16.05
MAR-M-509 Substrate	+40.00	+16.05

*Tensile stresses are positive
Compressive stresses are negative

GRADED ZrO_2-NiCr TURBINE SEAL

THERMAL & STRUCTURAL ANALYSIS (Cont'd)

Figure 6 shows that the axial direction stresses for this condition are within allowable limits using the newly measured mechanical properties of the graded ZrO_2-NiCr seal. Extrapolations from previous results show that at the full power condition compressive plastic flow will occur in the top 0.035 inches of ceramic, thus allowing tensile stresses to develop during cool-down, causing stable mud-flat cracking.

The "first modification" of the "initial" advanced engine graded ceramic turbine seal system has been thermally and structurally analyzed based on the then current design system which utilized the effects of surface radiation to other engine components as a result of continued improvement of the design system. Design modifications led to a further decrease of 0.19% W_{ae} in the total cooling air requirement. The resulting thermal distribution is given in Figure 7 for the most severe thermal (full power hot spot) condition after a 0.020 inch rub. All temperatures shown are below the allowable temperature limits, which is 1600°F for the metal bearing layers of the graded ZrO_2-NiCr seal. Structural analysis was performed throughout an engine operating cycle using a two-dimensional finite-element computer program, taking into account three-dimensional effects. The maximum principal stresses in the various seal layers throughout the cycle are given in Table II and are lower than the strength limits of the graded ZrO_2-NiCr seal at the anticipated engine operating conditions. Invariably these maximum principal stresses occur in the central portion of the seal relative to the edges. Shear stresses, highest near the edges, are not expected to present any problem, since they are well below the critical low cycle fatigue strain range. Compressive plastic flow at power was expected to cause mud-flat cracking in the top 0.050 inches of the ZrO_2 with some plastic flow in the top 0.067 inches. This mud-flat cracking is stable and will not lead to system failure, and, because of the high stiffness of the metal substrate, it will not lead to higher stresses in the ZrO_2 at any engine cycle condition.

The "second modification" of the "initial" advanced engine graded ZrO_2-NiCr turbine seal design initiated thermal and structural analysis of a seal concept that minimized number of segments with a reduction from 32 to 6. In addition the metal trailing edge was replaced with the graded ceramic layer.

The "final" advanced engine graded ceramic turbine seal design has been thermally and structurally analyzed. This ceramic turbine seal system incorporates 6 segments with graded ZrO_2-NiCr layer on the entire gas path surface. Each segment is a 60 degree arc made up of 3 component 20 degree arc segments welded together. All seal temperatures will remain within acceptable limits using $\approx$ 0.75% W_{ae} cooling air distributed as shown in the flow map (Figure 8). The resulting thermal distribution is given in Figure 9 for the most severe thermal condition (full power hot spot) after a 20 mil rub interaction has occurred.

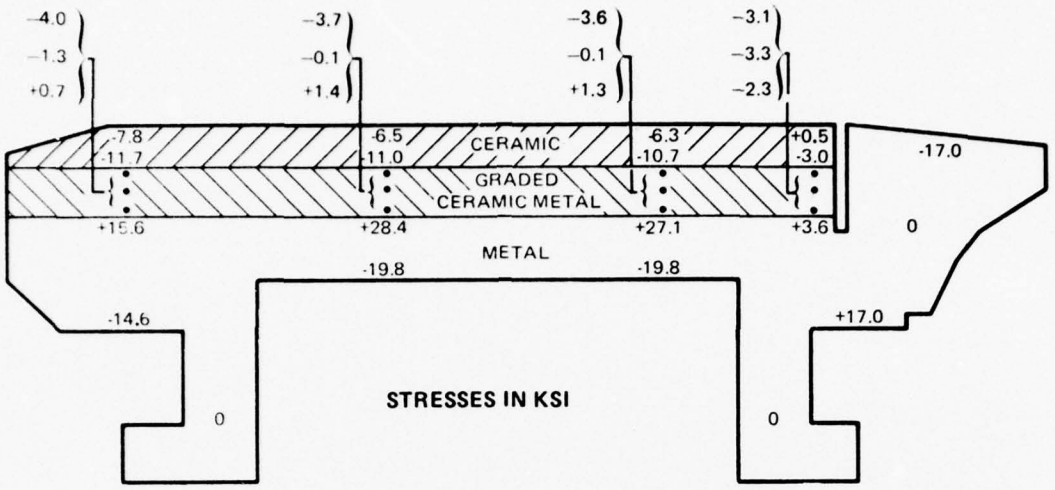

Figure 6 Axial Stress Map of the "Initial" Advanced Engine Graded ZrO_2-NiCr Turbine Seal Design at Room Temperature Condition After an .020 Inch Rub

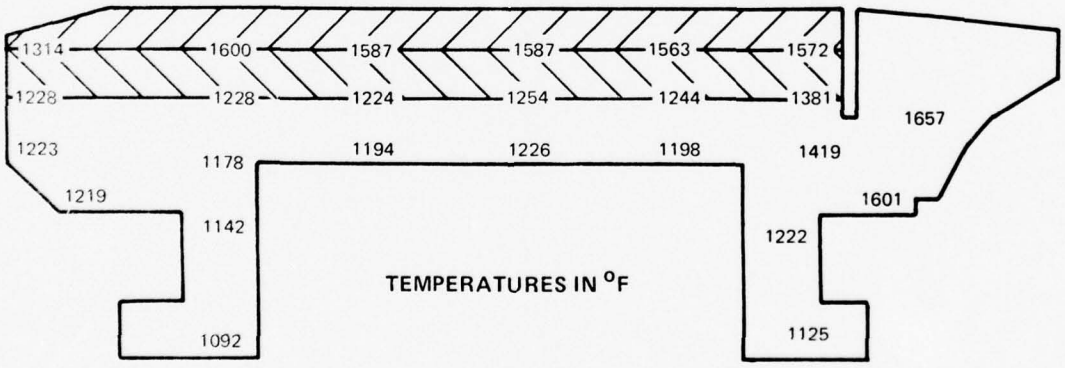

Figure 7 "First Modification" Advanced Engine Ceramic Seal Design Temperature Distribution at the Postrub Sea Level Takeoff Power Condition

TABLE II

ESTIMATED STRESS LEVELS FOR "FIRST MODIFICATION" ADVANCED ENGINE CERAMIC SEAL (STRESS IN KSI)

Seal Layer	Room Temperature	30-Second Start Up	Idle	6-Second Accel	Sea Level Takeoff	12-Second Decel
Ceramic	– 4.0	–14.5	– 9.0	– 9.0	– 5.5	– 6.0
Intermediate	– 9.9	–11.4	– 9.9	– 8.7	–10.4	–11.3
Metal	23	29	21	15	10	21

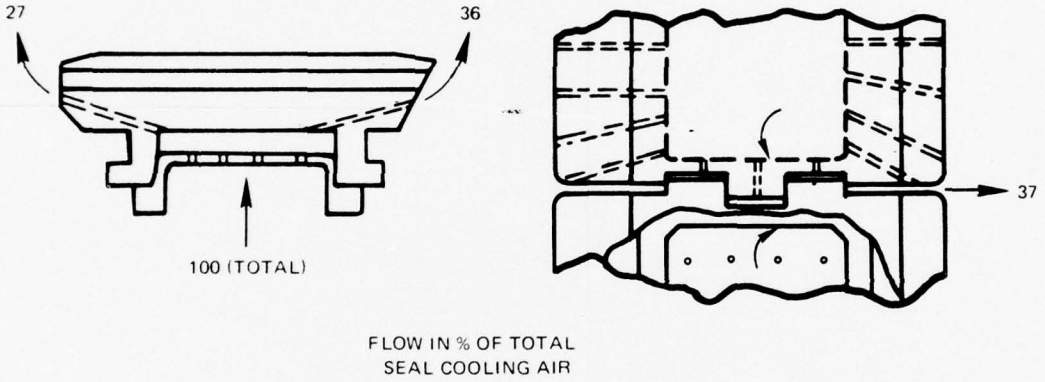

Figure 8 "Final" Advanced Engine Ceramic Seal Design Flow Map

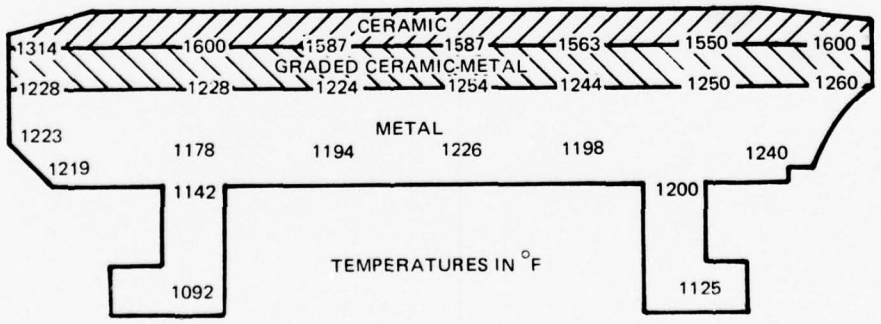

Figure 9 "Final" Advanced Engine Ceramic Seal Design Temperature Distribution at the Postrub Sea Level Takeoff Power Condition

GRADED ZrO_2-NiCr TURBINE SEAL

THERMAL & STRUCTURAL ANALYSIS (Cont'd)

Structural analysis was performed throughout an engine operating cycle using a two-dimensional finite element computer program, and accounting for three-dimensional effects with flat plate theory. A thermal gradient in-process stress relief cycle was utilized to produce a stress-free temperature of 800° F in order to optimize the engine cyclic stresses within the allowable ZrO_2-NiCr seal strength limits. The maximum principal stresses are given in Table III. Invariably, these maximum principal stresses occur in the central portion of the seal relative to the edges and are below the experimental strengths in every case. Shear stresses at the seal edges are insignificant compared to the principal stresses.

Compressive plastic flow at power is expected to cause mud-flat cracking in the top 45 mils of the ZrO_2. This mud-flat cracking is stable and will not lead to system failure. Mud-flat cracking is the result of creep occurring in the ceramic layer during the high temperature portion of the engine cycle. The creep is induced by the compressive stress existent in the ceramic, which leads to a negative strain in those portions of the ceramic where the temperature exceeds the creep temperature. During cooldown portions of the ceramic are forced into tension, and in the locations where the tensile stress exceeds the ultimate strength mud-flat cracking occurs. The mud-flat cracking is stable since the ceramic relieves itself by reducing the maximum stress below the ultimate strength level.

Structural analysis predicts that the corners of the seal will deflect radially outward approximately 0.013 inches relative to the center during the fabrication cycle. This distortion has been dimensionally accounted for during design. Table IV shows the deflections predicted for the seal through the operating cycle relative to room temperature, and are considered minor.

TABLE III

ESTIMATED STRESS LEVELS FOR "FINAL" ADVANCED ENGINE CERAMIC SEAL (STRESS IN KSI)

Seal Layer	Room Temp.	30 Second Start Up	Idle	6 Second Accel.	Sea Level Take-off	12 Second Decel.
Ceramic	-5.4	-6.2	-0.3	-7.5	-5.1	-3.2
Intermediate	-2.3	-3.7	-3.8	-2.8	-4.5	-7.4
Metal	+15	+20	+14	+10	+7	+14

TABLE IV

PREDICTED MAXIMUM OPERATING DEFLECTIONS* FOR "FINAL" ADVANCED ENGINE CERAMIC SEAL

	30 Second Warmup	Idle	6 Second Accel.	Sea Level Takeoff	12 Second Decel.
Deflection (mils)	1.0	–	2.8	−0.4	−3.6

*Relative to Room Temperature (Axial)

GRADED ZrO_2-NiCr TURBINE SEAL

FABRICATION QUALITY CONTROL

NDT inspection analysis indicates that revised fabrication techniques have resulted in significantly improved specimens for the "first modification" and "second modification" test iterations.

Fabrication quality control utilized in manufacturing the "initial" graded ZrO_2-NiCr rig seals has resulted in samples with large variations in overall mean coating hardness, individual specimen hardness, and structure uniformity (see page 16).

Thermal fatigue, erosion, and rub rig specimens evaluated during this testing iteration, while only slightly lower in average hardness, exhibited a significantly inferior hardness spectrum compared to Phase II specimens, as indicated by the increased percentage of specimens with large minimum/maximum hardness range (Figure 1). Also, a significant decrease in hardness was identified after thermal cycling the rub test specimens (see page 31, Table X). Consideration of the "initial" iteration test results, discussed in the Rig Specimen Testing section, has shown that minimum/maximum hardness range can be utilized for determination of fabrication quality.

X-ray data can detect variations in thickness and density, internal cracks, voids, and braze defects. Therefore, X-ray inspection can be utilized for improved fabrication control.

Prior to fabrication of the "first modification" test specimens, extensive effort was expended on improvement of fabrication techniques to minimize dependence on handcrafting. In particular, the objectives of this effort were: to eliminate laminar defects; to maintain an average specimen hardness of 65 to 75 (RS45Y); and to maintain a minimum-to-maximum hardness range of 15 on each specimen.

A series of experiments were performed to resolve the quality control problems previously experienced. The experiments included varying of mixing, forming and bonding parameters. X-ray and hardness inspection is being utilized to evaluate the effect of parameter variation. The evaluations were conducted on specimens in the green state, fired state, and thermal stress relieved condition. X-ray analysis has determined that defects such as density variation and laminar separations do not heal during processing. However, mechanical fixes have essentially eliminated defects in the green state and additional process steps have not created defects.

Specimens for the "first modification" and "second modification" of the "initial" seal design were fabricated with the improved mechanical fixes for the green state fabrication. Examination of these rig seal specimens using visual, microscopic, X-ray, and hardness techniques revealed a significant decrease in the quantity and severity of fabrication defects of the types that have been associated with specimen failure, as seen in Tables IV, V, VII, and VIII in the Nondestructive Inspection section, Figure 2. This improvement has been realized as a result of the experiments performed. The most common imperfection found, (Tables IV and V) was a density variation in the intermediate layer.

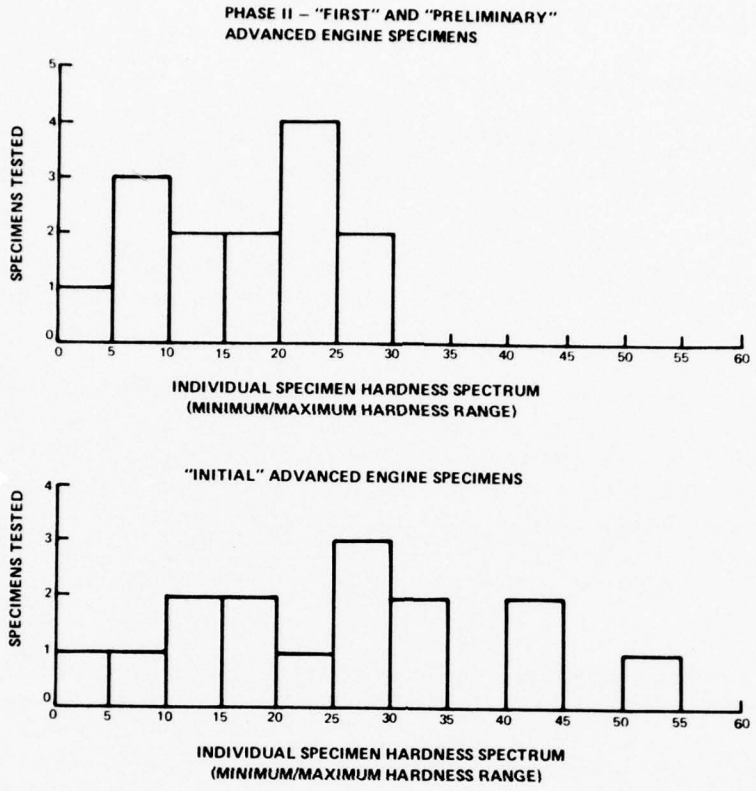

Figure 1 Graded Ceramic Hardness Data

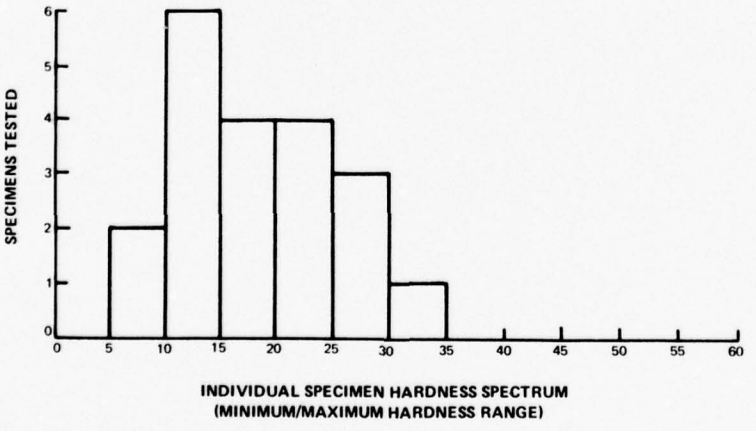

Figure 2 Graded Ceramic Hardness Data for "First Modification" and "Second Modification" Advanced Engine Specimens

GRADED ZrO_2-NiCr TURBINE SEAL

RIG SPECIMEN TESTING & ANALYSIS

The graded ZrO_2-NiCr advanced engine turbine seal thermal fatigue, erosion and rub tests have demonstrated that the graded ZrO_2-NiCr seal system can exceed the performance requirements with thermal fatigue life greater than 500 cycles, erosion life greater than 1600 hours for 10 mils and rub tolerance that produces 10 mils of seal wear for less than 1 mil of *average blade wear.*

THERMAL FATIGUE

The thermal fatigue specimen design shown in Figure 1 was intended to closely simulate the engine construction features and was used for the "first" and "preliminary" iterations test phases. All thermal fatigue tests were set up to impose a cycle closely simulating the thermal conditions predicted for the engine seals as discussed in detail in the Thermal and Structural Analysis section on page 7.

The first graded ZrO_2-NiCr seal specimen was tested in the "as-fabricated" condition. The test was terminated after 150 cycles due to severe cracking of the top layer as shown in Figure 2. Macroscopic examination showed that the graded ZrO_2-NiCr layer had delaminated about 20 mils above the substrate interface and bowed upward at the center. Significant discoloration of the graded ZrO_2-NiCr layer was apparent which strongly indicates gross oxidation of the NiCr.

Modifications were made to the thermal fatigue rig due to inadequacies in the test set up and controls that allowed excessive temperature of the intermediate layer which caused premature failure. These modifications include improved controls, non-restricting heat shield and a flexible mounting system.

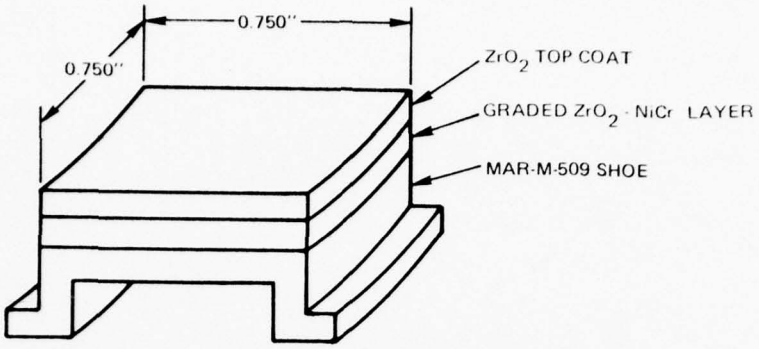

Figure 1 Graded Ceramic-Metal Thermal Shock Specimen

Figure 2 Graded ZrO_2-NiCr Rig Specimen After 150 Thermal Fatigue Cycles Tested In "As-Fabricated" Condition

GRADED ZrO_2-NiCr TURBINE SEAL

RIG SPECIMEN TESTING & ANALYSIS (Cont'd)

As part of the "first" design evaluation, two additional rig specimens were isothermally pre-aged for 100 hours at 1600°F and 1800°F, respectively, to determine the effect of oxidation on thermal fatigue life of the graded ZrO_2-NiCr seal system. Macroscopic examination of 1600°F specimen after aging (Figure 3) showed that it had a minor surface crack across approximately 1/3 of the sample that extended to the intermediate graded ZrO_2-NiCr layer at one edge connecting to a laminar crack at the intermediate-top coat interface. The 1600°F specimen completed 203 thermal fatigue cycles before the test was terminated due to delamination of approximately 1/6 of the ZrO_2 layer at the graded layer interface (Figure 4). Macroscopic examination of the sample after thermal fatigue testing indicated that approximately 1/3 of the ZrO_2 layer remained bonded to the intermediate layer and that the mud-flat cracking was much less severe than that evidenced in the "as-fabricated" thermal fatigue specimen tested. The 1800°F specimen delaminated approximately 20 mils above the substrate interface in the graded ZrO_2-NiCr layer during the 1800°F, 100 hour isothermal aging process and therefore was not thermal fatigue tested.

The "preliminary" advanced engine graded ZrO_2-NiCr seal thermal fatigue rig specimens were tested in the "as fabricated" configuration at hot spot surface temperatures predicted for the advanced engine cycle. The first specimen survived 503 thermal fatigue cycles before delamination failure caused termination of the test. The second thermal fatigue specimen test was terminated after 33 cycles due to delamination in the top layer approximately 20 mils above the intermediate layer interface. As a result of this early failure the remaining thermal fatigue specimens were subjected to extensive microscopic examination. Pretest surface and laminar cracks were noted in these specimens in the general location of the failure. While the cause of these cracks is not known, a strong possibility exists that they were induced during cutting from the full size specimens. As expected, the third specimen failed prematurely along the pretest faults after 69 cycles.

The thermal fatigue specimen configuration was modified for the "initial" test phases to be identical with the rub rig specimens (Figure 5) to more closely simulate engine stresses in the graded ZrO_2-NiCr turbine seal. Analysis performed during Phase II indicated that the 3/4-inch square segment could result in excessively high internal stresses. The rub rig specimen configuration creates stresses in the coating more nearly simulating stress which would be generated throughout a full engine operating cycle.

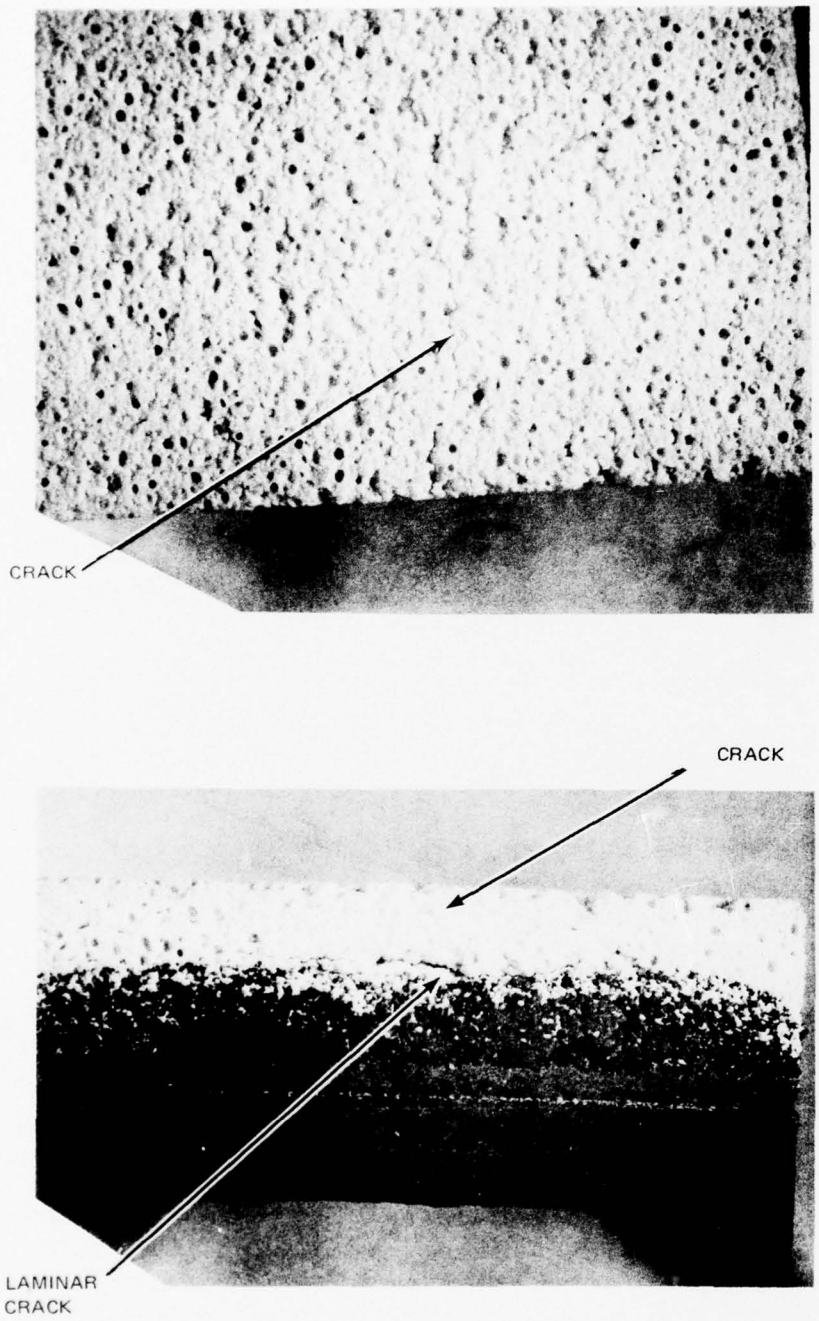

Figure 3 Graded Ceramic-Metal Seal Specimen After Isothermal Aging for 100 Hours at 1600°F

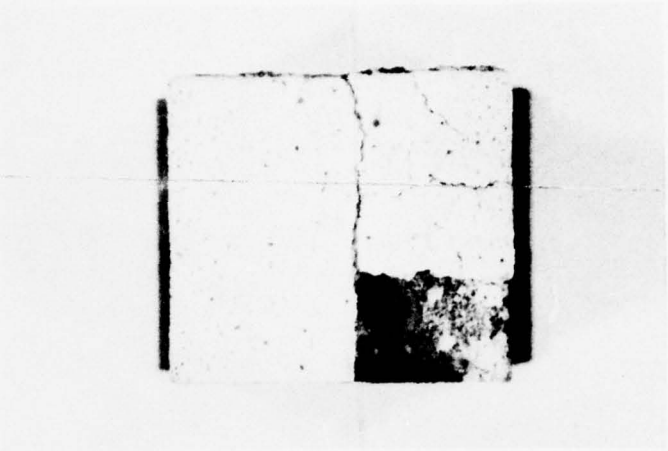

Figure 4 Graded Ceramic-Metal Seal Specimen (Preaged 100 Hours at 1600°F) After 203 Thermal Fatigue Cycles

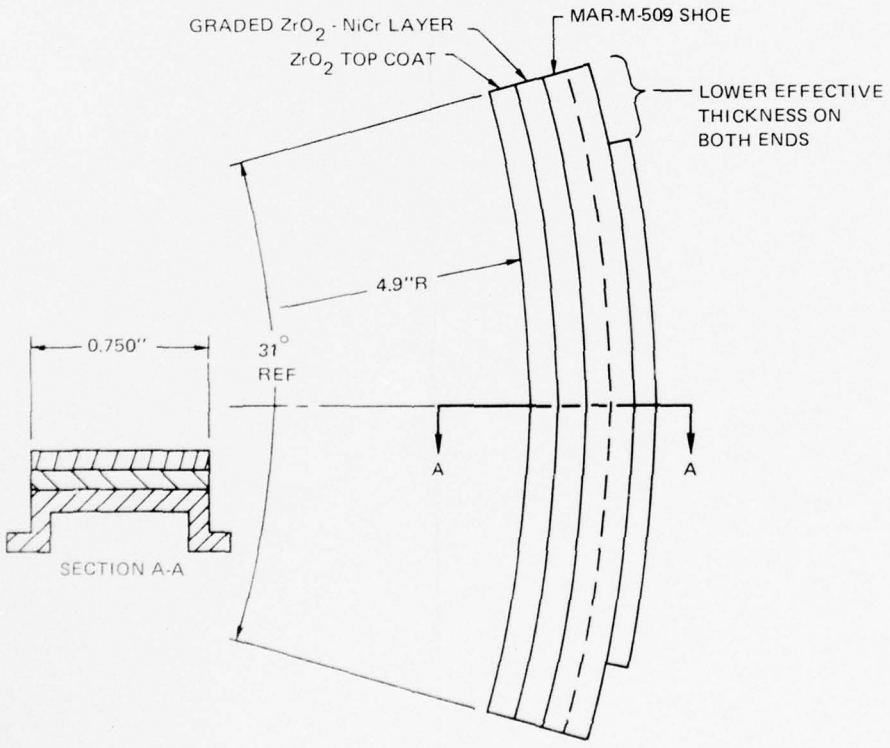

Figure 5 Graded Ceramic-Metal Rub Specimen

GRADED ZrO_2-NiCr TURBINE SEAL

RIG SPECIMEN TESTING & ANALYSIS (Cont'd)

The results of "initial" advanced engine graded ZrO_2-NiCr rig tests are summarized in Table I. The cyclic life of these test specimens was lower than anticipated, approximately 50 percent less than in Phase II testing. This has been identified as a serious quality control problem. Quality control problems are discussed in detail in the Fabrication Quality Control section on page 15.

Three improved quality "first modification" graded ZrO_2-NiCr rig seal specimens were tested for thermal fatigue characteristics in the "as fabricated" condition. The results, summarized in Table II indicate a significant improvement over previous testing with one specimen surviving 917 cycles before minor spallation, approximately twice the cyclic life of the best advanced engine specimen to date. The other two specimens, tests of which were terminated prior to failure, exhibited continuous broadening of cracks near the circumferential ends similar to the occurrences that progressed to delamination failure of the 917 cycled specimen. The circumferential ends were also the hot spot areas during test. The crack broadening is postulated to occur from swelling of the intermediate layer, caused by oxidation due to overtemperature, which in turn is caused by failure in the intermediate layer. Laboratory analysis for the degree and location of intermediate layer oxidation has been performed as discussed in the Materials Analysis Tested Rig Specimen section on page 41 supports this postulation.

Detailed analysis of the test specimens indicates that the metal substrate at the ends has a lower effective thickness which will result in unacceptable tensile stresses in the intermediate layer during the acceleration portion of the test cycle. These predicted tensile stresses are the probable initial cause of the current thermal fatigue testing failure.

TABLE I

RESULTS OF THERMAL FATIGUE TESTING OF THE "INITIAL" ADVANCED ENGINE SEAL DESIGN

Test Number	Total Thermal Fatigue Cycles to Failure	Shutdown Cycles
1	252	6
2	183	6
3	208	7

TABLE II

THERMAL FATIGUE TEST RESULTS FOR "FIRST MODIFICATION" OF THE "INITIAL" ADVANCED ENGINE SEAL DESIGN

Test Number	Total Thermal Fatigue Cycles	Shutdown Cycles
1	917	14
2	500*	7
3	620*	7

*Test terminated prior to failure

GRADED ZrO_2-NiCr TURBINE SEAL

RIG SPECIMEN TESTING & ANALYSIS (Cont'd)

The "second modification" graded ZrO_2-NiCr thermal fatigue rig seals fabricated using the improved mixing, forming and bonding techniques were machined to remove the portion of the specimen ends that were of lower effective thickness (Figure 5) prior to test. The results of these tests, shown in Table III, continue to show the significant improvement obtained in the "first modification" testing. During previous tests the rig controls have normally required adjustment in the first 50 to 150 cycles to maintain the desired thermal conditions implying the initiation of cracks. In the test of specimen Number 3, which was the best from NDT evaluation, adjustments were unnecessary for approximately 350-400 cycles demonstrating further improvement in thermal fatigue performance. Figure 6 shows the condition of this specimen during test after 410 cycles. Specimen 1 and 2 which had some low density at the ends in intermediate layer were subjected to over 850 cycles before delamination.

TABLE III

THERMAL FATIGUE TEST RESULTS
"SECOND MODIFICATION" ADVANCED ENGINE CERAMIC TURBINE SEAL

Test Number	Total Thermal Fatigue Cycles	Shutdown Cycles
1	864	19
2	881	22
3	607*	9

*Test terminated prior to failure

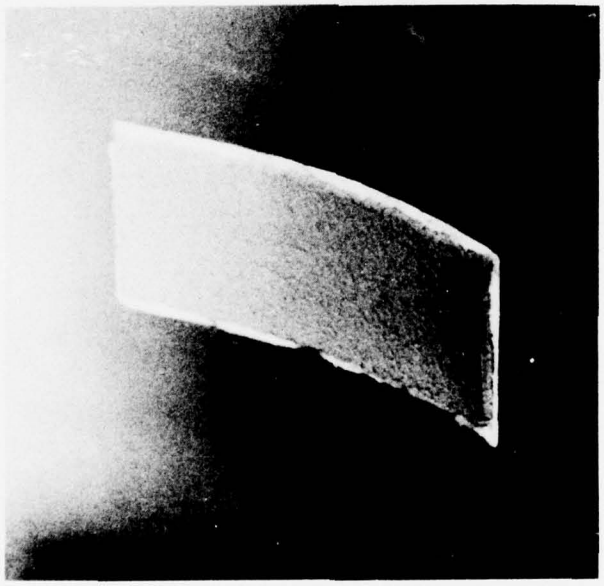

Figure 6 Graded Ceramic-Metal Thermal Fatigue Specimen at 410 Cycle – Idle Condition

GRADED ZrO_2-NiCr TURBINE SEAL

RIG SPECIMEN TESTING & ANALYSIS (Cont'd)

EROSION

Hot gas erosion specimens (Figure 7) were designed to simulate engine seal cross-sectional construction to determine experimentally the surface durability or life at engine predicted temperatures. During Phase II and Phase III all specimens were erosion tested at temperatures between 2850 and 3200°F with Mach 0.8 gas velocity in air at atmospheric pressure.

Erosion lives determined from the test results (Figure 8) of the "first" advanced engine graded ceramic-metal rig specimens were considered exceptional for this point in the development cycle. Calculations of the erosion rates are based on the steady state portion of the weight-loss curves, the measured impingement area on the specimens, and the density of the ZrO_2 layer of the seal coatings.

Hot gas erosion data from the "preliminary" rig tests indicate that erosion is a function of the coating superficial hardness. Hardness dependent erosion lives were obtained (Table IV for each of the specimens tested at 2850°F. The hardness data presented in Table IV was measured using a Rockwell Rs45Y superficial hardness tester. The erosion life of the hardest specimen correlates well with the results of the "first" graded ZrO_2-NiCr rig tests as shown in Figure 9.

Erosion test of two "initial" graded ZrO_2-NiCr specimens were completed with the "as-fabricated" ceramic surface finish (nominally 560AA). The third specimen was ground to a nominal 160 AA roughness to evaluate the effect of surface finish. The results of testing at 2890°F are summarized in Table V. The inferior erosion life and failures experienced in this testing, that did not occur in any other test phase, are attributed to fabrication quality control which was identified as a prime problem and is discussed on page 15 and precluded determination of surface finish effect.

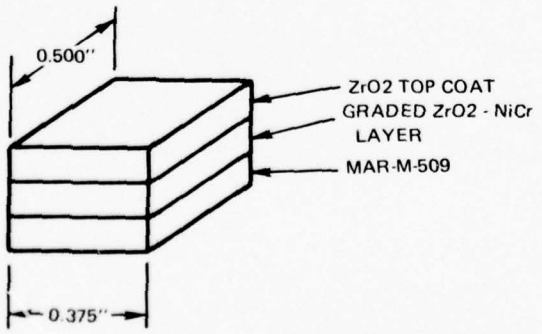

Figure 7 Graded Ceramic-Metal Erosion Specimen

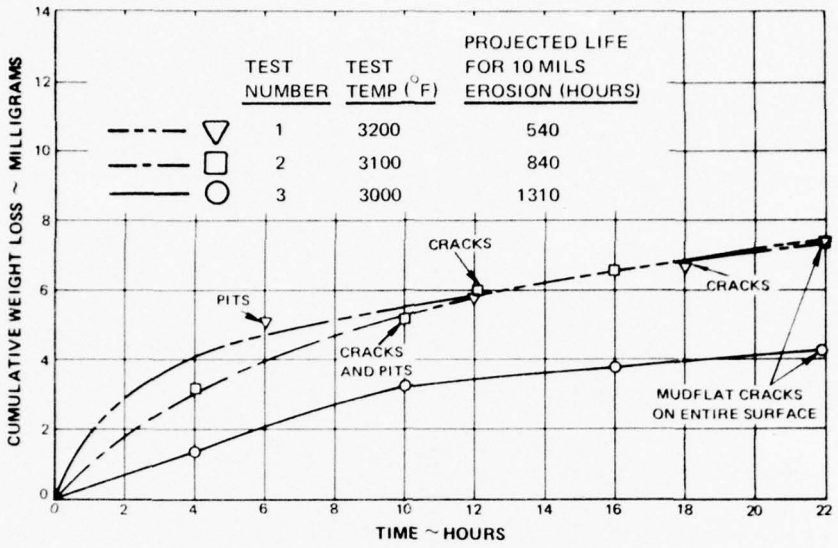

Figure 8 Results of Hot Gas Erosion Testing of the Graded ZrO_2-NiCr Seal Specimens

TABLE IV

RESULTS OF EROSION TESTING OF THE "PRELIMINARY" ADVANCED ENGINE SEAL DESIGN

Test Number	Erosion Life Hrs/10 Mils	Rs45Y Hardness (Average) "As-Fabricated"	Post-Test*
1	926	50	29
2	603	–	10
3	2860	65	61

*Surface Machined Approximately 20 Mils After Erosion Test.

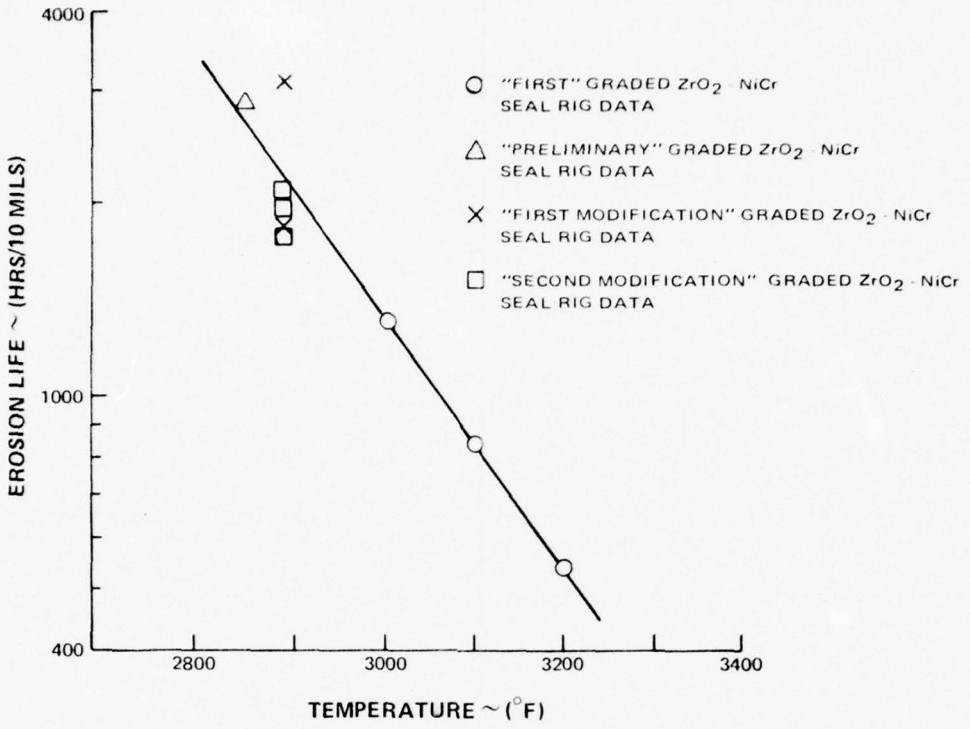

Figure 9 Graded ZrO_2-NiCr Seal Thermal-Erosion Life Correlation

TABLE V

RESULTS OF EROSION TESTING OF THE "INITIAL" ADVANCED ENGINE SEAL DESIGN

Test Number	Test Time (Hours)	Time for 10 Mils Erosion (Hours)
1*	17	936
2	10.5	**
3	29	1147

*Surface machined to a nominal 160 AA finish.
**Complete delamination occurred.

GRADED ZrO_2-NiCr TURBINE SEAL

RIG SPECIMEN TESTING & ANALYSIS

EROSION (Cont'd)

Results of erosion test of the "first modification" graded ZrO_2-NiCr specimens (Table VI) are significantly improved over the "initial" iteration erosion lives although inconsistent weight loss data resulted in a wide range for predicted erosion life. Lack of consistency has been attributed to two primary variations from prior testing: 1) substrate effective thickness, and 2) ceramic surface preparation. Current test specimens were fabricated on substrate backings with an effective thickness of 0.100 inch as compared to a previous thickness of 0.190 inch. The 0.100 inch effective thickness is analytically predicted to cause problem tensile stresses to which prior erosion specimens (0.190 inch thickness) were not subjected. Secondly, since the current erosion specimens were fabricated from flat stock, and not the rub specimen configuration, the ceramic surface was prepared differently from prior erosion specimens. This superficial ceramic surface preparation produced a coarser surface finish than prior diamond grinding.

The "second modification" erosion specimens were fabricated on substrate backing with an effective thickness of 0.190 inch and the surface was diamond ground to prevent problems experienced in the "first modification" tests. All the fabrication improvements discussed have produced a ceramic layer that has a reproducible minimum life of 1600 hours for 10 mils of erosion as indicated in Table VII which are very consistent.

TABLE VI

EROSION TEST RESULTS FOR THE "FIRST MODIFICATION" OF THE "INITIAL" ADVANCED ENGINE SEAL

Test Number	Test Time (Hours)	Time for 10 Mils Erosion (Hours)
1	48	3100
2	33	1640
3	22	*

*Equilibrium erosion rate not determined due to inconsistent weight loss data.

TABLE VII

EROSION TEST RESULTS FOR THE "SECOND MODIFICATION" ADVANCED ENGINE CERAMIC TURBINE SEAL

Test Number	Test Time (Hours)	Time for 10 Mils Erosion (Hours)
1	34.5	2039
2	37	1612
3	37	1697

GRADED ZrO_2-NiCr TURBINE SEAL

RIG SPECIMEN TESTING & ANALYSIS (Cont'd)

RUB TOLERANCE

Rub rig test specimen design, shown in Figure 5 for the graded ZrO_2-NiCr seals, which closely simulates engine seal construction features, was used for all abradability testing.

An important consideration in establishing a rub tolerant turbine ceramic seal system is parallel development of blade tip treatment. To improve system abradability (decreased blade wear), an abrasive tip treatment is being developed by P&WA under AFML Contract F33615-75-C-5048 for utilization with this seal design.

Ambient temperature rub tests were conducted on two "first" advanced engine graded ZrO_2-NiCr seal specimens (samples A and B) using a blade tip treated with 25-mil (nominal diameter) silicon carbide abrasive grits totally encapsulated in nickel plate (Table VIII). The test conditions closely simulate the predicted advanced engine first-stage turbine rotor at full power rotor speeds and interaction rates. The graded ZrO_2-NiCr seals exhibited excellent wear characteristics in these rub tests with the silicon carbide grits, as indicated by the extremely low volume wear factor (VWF), 1×10^{-5} average (Table VIII). The high temperature test on a third specimen (sample C, Table VIII) was run at 2500°F seal surface because of an imposed test limit of 2150°F on the MAR-M-509 substrate. A premature rub occurred while the temperature and speed conditions were being set. After clearance adjustments the test was run to a total depth of approximately 20 mils. The graded ZrO_2-NiCr specimen exhibited some grooving, spalling, metal transfer and heavy oxidation. All of the silicon carbide grits on the blade tip were missing after the test.

During the test phase of the "preliminary" advanced engine ceramic seal design evaluation, all rub testing was done using a blade tip treatment consisting of 25 mil diameter SiC grits vacuum hot pressed (VHP) in an M-CrAlY matrix. One rub test performed at room temperature produced a uniformly grooved seal without blade tip matrix material transfer. The VWF was 5.56×10^{-5}. High temperature rub tests conducted on two seal specimens produced grooving of the seals by the blade tip treatment. In the first high temperature rub test (Table IX) an inadequate braze bonded blade tip treatment experienced excessive thermal growth causing premature interaction. The result was seal grooving, transfer of blade tip matrix material and the loss of the abrasive tip treatment by debonding at the braze interface. The second high temperature rub test (Table IX) also produced grooving of the seal and transfer of the blade tip matrix material with a VWF approximately one order of magnitude higher than the room temperature test using the same blade tip treatment system. The occurrence of metal transfer normally results in high blade tip wear.

The VWF reported for rub tests using VHP tip treatments were evaluated using a more encompassing "total blade tip" method instead of the original individual grit wear analysis due to the larger number of active grits. This change produces a VWF in the range of 0.01 as compared to 5×10^{-5}.

All Phase III rub tests were conducted with blade tip rotational speed of 1000 feet per second and a rub interaction rate of 1 mil per second.

During the "initial" advanced engine test phase, four rub abradability tests were conducted using 25-mil-diameter SiC-grit/M-CrAlY compact tip treated rig blades. Tests were conducted both at room temperature and at 2900°F for total rub interaction depts of 20 to 25 mils.

TABLE VIII

RESULTS OF RUB TESTING OF THE "FIRST" ADVANCED ENGINE GRADED ZrO_2-NiCr SEAL SPECIMENS

Test Number	Rub Speed (ft/sec)	Seal Temp. (°F)	Interaction Rate (in/min)	Average VWF[a]
1	1500	RT	0.0027	1.5×10^{-5}
2	1500	RT	0.0054	6×10^{-5}
3	1317	2500	0.0027	b

a. Volume wear factor (VWF) is equal to the blade tip wear volume divided by the seal wear volume.
b. Grits debonded during test.

TABLE IX

RESULTS OF RUB TESTING "PRELIMINARY" ADVANCED ENGINE CERAMIC SEAL SPECIMENS

Test Number	Rub Speed (ft/sec)	Seal Temp. (°F)	Interaction Rate (in/min)	Average VWF[a]
1	1000	RT	0.004	0.01
2	763	2500	> 0.030[b]	b
3	1013	2700	0.0054	0.32

a. Volume wear factor (VWF) is equal to the blade tip wear volume divided by the seal wear volume.
b. Poor braze bond caused excessive tip growth, premature interaction and loss of blade tip treatment.

GRADED ZrO_2-NiCr TURBINE SEAL

RIG SPECIMEN TESTING & ANALYSIS

RUB TOLERANCE (Cont'd)

Rub instabilities were found in all test specimens with or without prior simulated engine thermal fatigue cycling. The instabilities produced various failures that did not allow VWF to be determined (Table X). Rub instabilities identified for the ceramic coating were classified as spallation of surface material, delamination of the all-ceramic layer, and a more complex, intermediate wear mode that included seal grooving in conjunction with surface spallation. These wear mechanisms are depicted in Figure 10.

Tests 1 and 2 illustrate the effect of inadequate ZrO_2-to-intermediate-layer bond, which was not observed in Phase II testing. Tests 3 and 4 depict the effect of ZrO_2 with inferior strength, which also was not experienced in Phase II testing. The defects associated with the four tests are definite fabrication quality problems as noted by nondestructive testing. The quality control problems are discussed in detail on page 15.

TABLE X

RESULTS OF RUB TESTING THE "INITIAL" ADVANCED ENGINE SEAL DESIGN

Test Number	Average Seal Hardness (Rs45Y)	Min/Max Seal Hardness Range (Rs45Y)	Seal Temp. (°F)	Seal Wear (inch)	Blade Tip Wear (inch)
1[a]	67 (18)[b]	30	Room temp.	Ceramic coating spallation	0.0006
2	62	17	2900	Ceramic coating delamination	< 0.001
3	48	15	Room temp.	0.006 plus spallation	0.027[c]
4[a]	56 (34)[b]	43	Room temp.	0.0175 plus spallation	0.0015

a. Seal coating subject to five advanced engine thermal cycles prior to rub.
b. Seal hardness after five advanced engine thermal cycles.
c. Blade tip treatment failure.

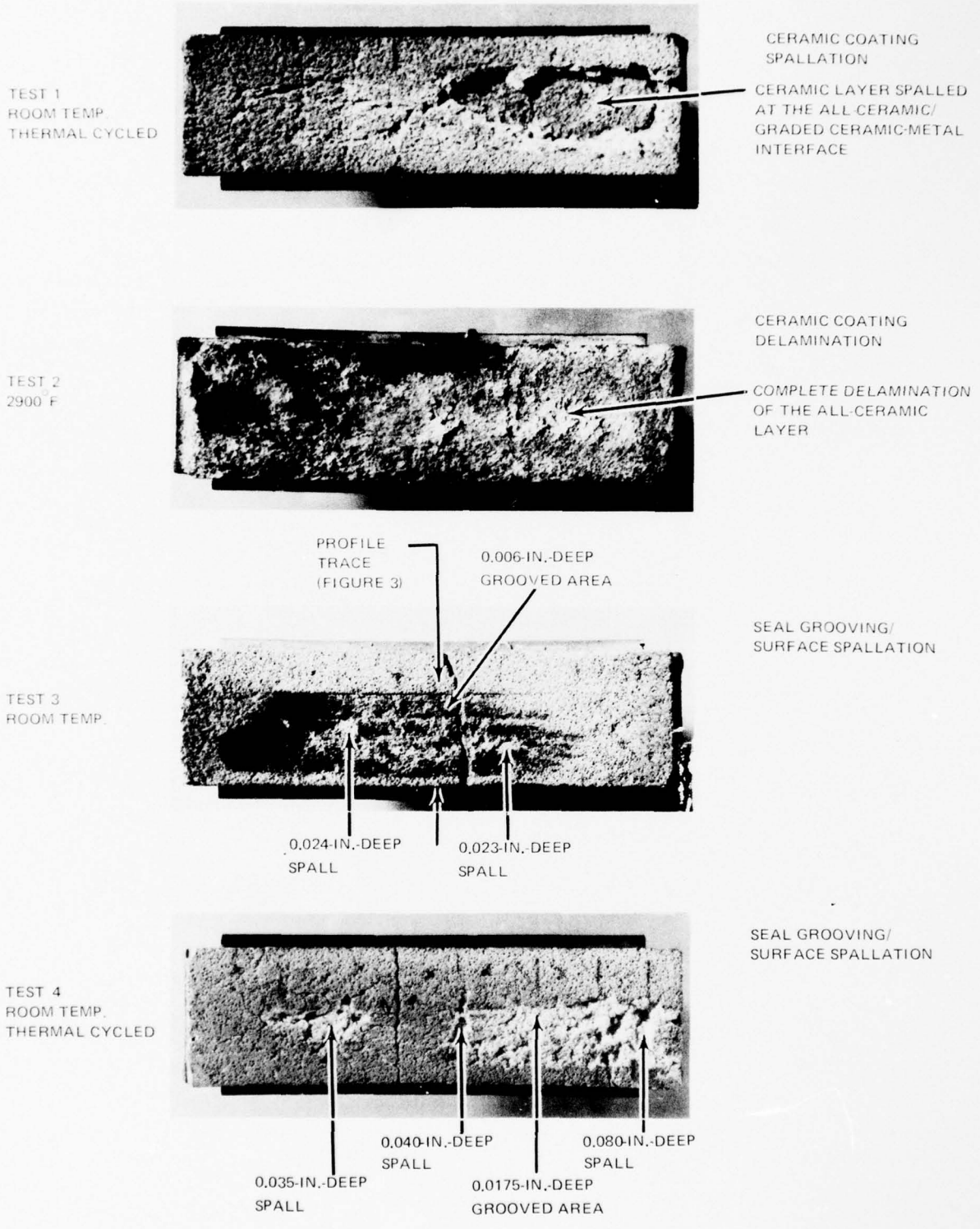

Figure 10 "Initial" Rub Test Wear Mechanism Identification

Figure 11 is a profilometer measurement of the rub and spallation surface depth.

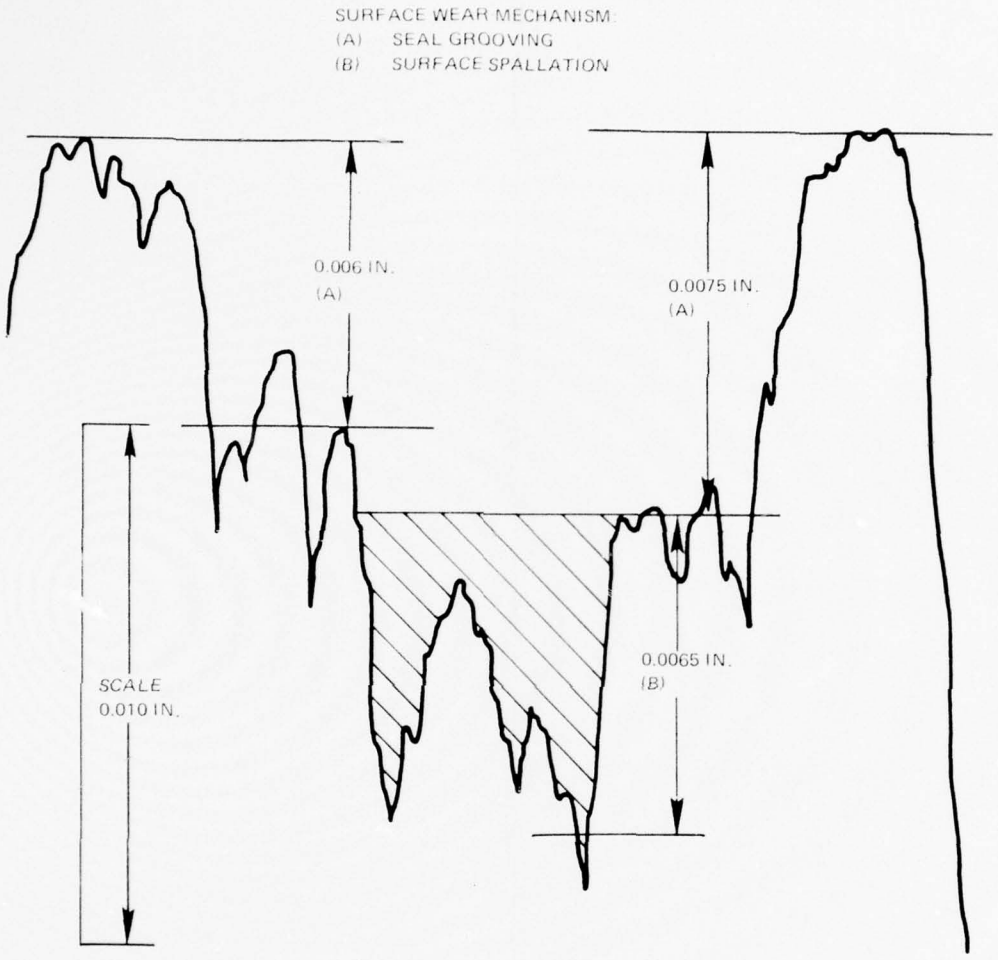

Figure 11 Rub Stability – Profile Trace of "Initial" Rub Abradability Test Specimen No. 3

GRADED ZrO_2-NiCr TURBINE SEAL

RIG SPECIMEN TESTING & ANALYSIS

RUB TOLERANCE (Cont'd)

During the rig test phase of the "first modification" advanced engine seal system, four abradability tests were conducted utilizing several blades with the most advanced state-of-the-art abrasive tip treatment. Multi-bladed rig tests more closely simulate the engine rub frequency and provide a foundation for engine correlation. The test results are summarized in Table XI. Various rub mechanisms identified by these tests are shown in Figure 12.

The "first modification" rub tests demonstrated the improved quality of the graded ZrO_2-NiCr seals, indicated by NDI as discussed in the Material Characterization section. Elimination of gross failures such as debonding, delamination, or spallation of significant areas of ceramic has resulted in improved and more meaningful abradability data.

TABLE XI

RESULTS OF RUB TESTING FOR THE "FIRST MODIFICATION" ADVANCED ENGINE SEAL

Test Number	Active Blades	Average Seal Hardness (Rs45Y)	VWF[a]
1	1	69	0.06
2	2	69	0.03
3	3	72	0.05
4[b]	1	65	0.01

(a) Calculated prior to blade tip transfer.
(b) Seal coating subjected to five advanced engine thermal cycles.

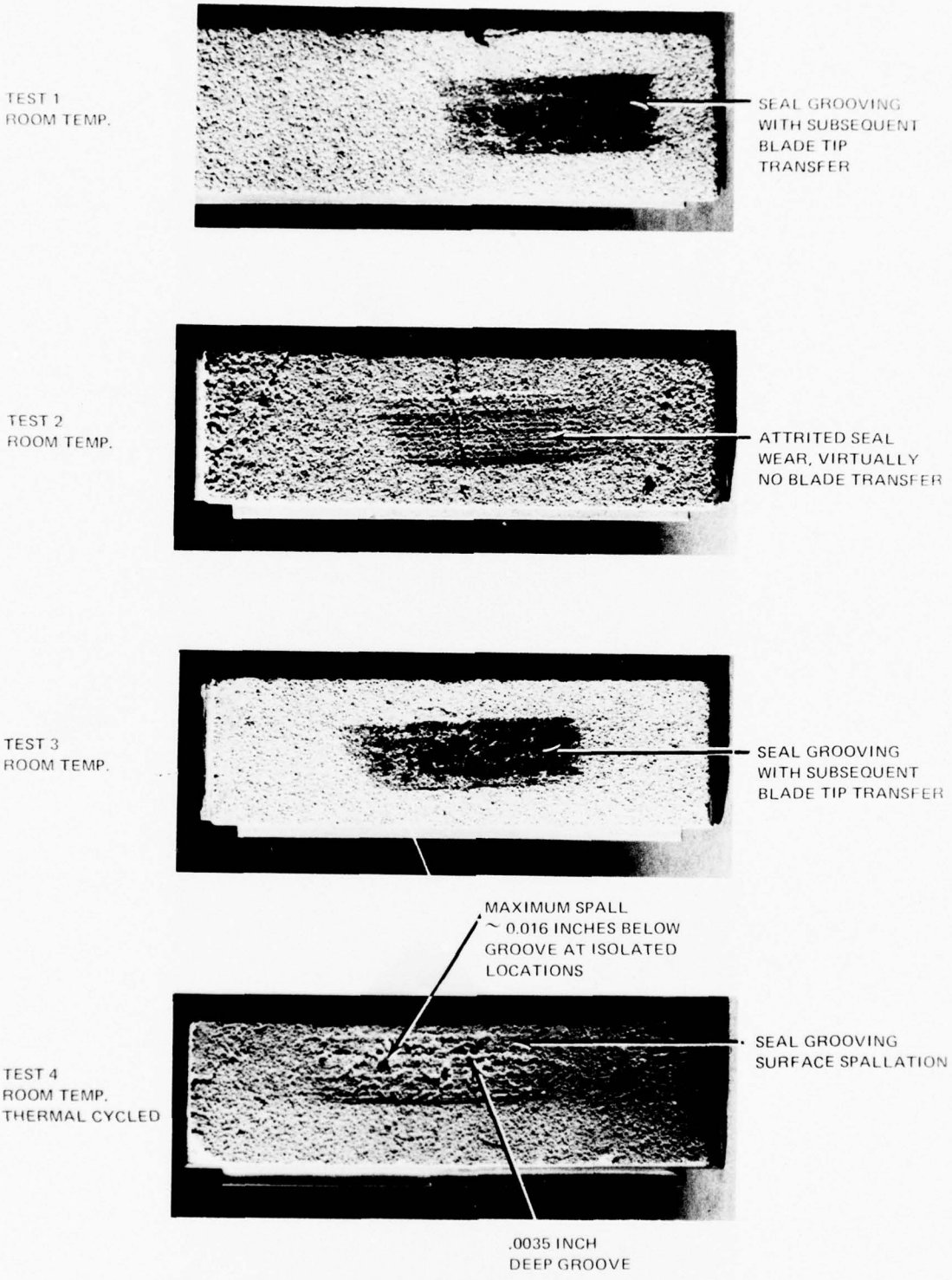

Figure 12 "First Modification" Rub Test Wear Mechanism Identification

GRADED ZrO_2-NiCr TURBINE SEAL

RIG SPECIMEN TESTING & ANALYSIS

RUB TOLERANCE (Cont'd)

During the rig test phase of the "second modification" advanced engine seal system, four multi-bladed abradability tests were conducted utilizing blades with the most advanced state of the art abrasive tip treatment. The test results are summarized in Table XII. Various rub mechanisms are classified in Figure 13.

Test No. 1 was run with blade tips with three holes in each simulating engine cooling hole geometry. Closure of the blade tip cooling holes was minimal (10-15%) as indicated in Figure 14. VWF of 0.045 was approximately the same as for tests without holes in the blade tips.

The "second modification" rub tests evaluated at advanced engine cycle temperatures revealed the improved seal durability and structural integrity of the closed cell seal system. The overall consistency of VWF (Table XII) has also indicated the improved quality control of the seal system.

Using "second modification" VWF data, an interaction in the advanced engine between the graded ZrO_2-NiCr turbine seals and the most advanced state-of-the-art tip treated blades is predicted to produce 10 mils of seal wear with less than 1.0 mil of average blade wear assuming 30% of the seal circumference is rubbed.

TABLE XII

RESULTS OF RUB TESTING FOR "SECOND MODIFICATION" ADVANCED ENGINE SEAL

Test Number	Seal Temp. (°F)	Active Blades	Average Seal Hardness Rs45Y	VWF[a]
1	RT	2-3	73.1	0.045
2	RT	4	71.5	0.036
3[b]	2900	3	64.5	0.021
4[b]	2900	3	74.6	0.085

(a) Calculated prior to blade tip transfer
(b) Tested at advanced engine cycle temperatures

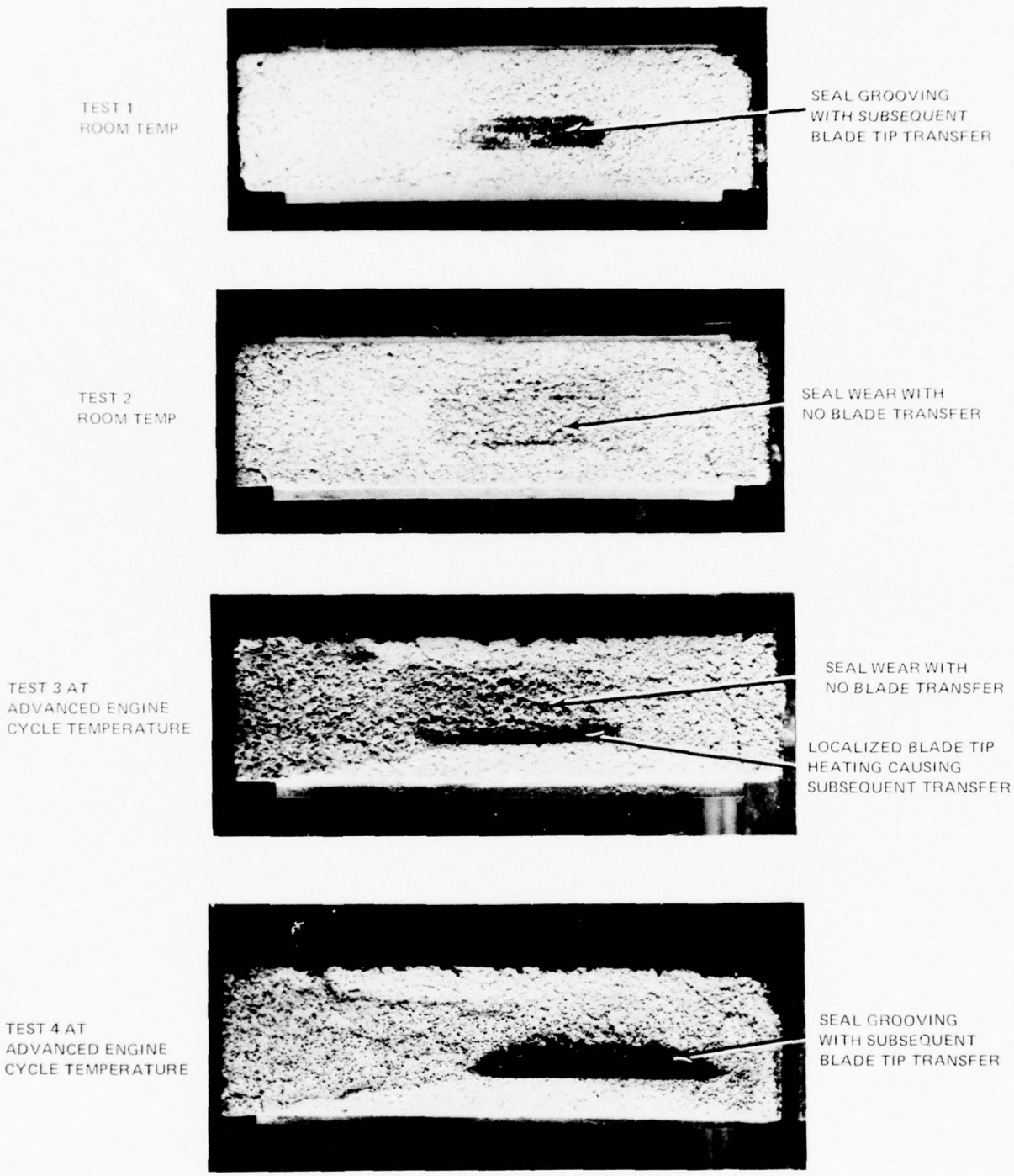

Figure 13 "Second Modification" Rub Test Wear Mechanism Identification

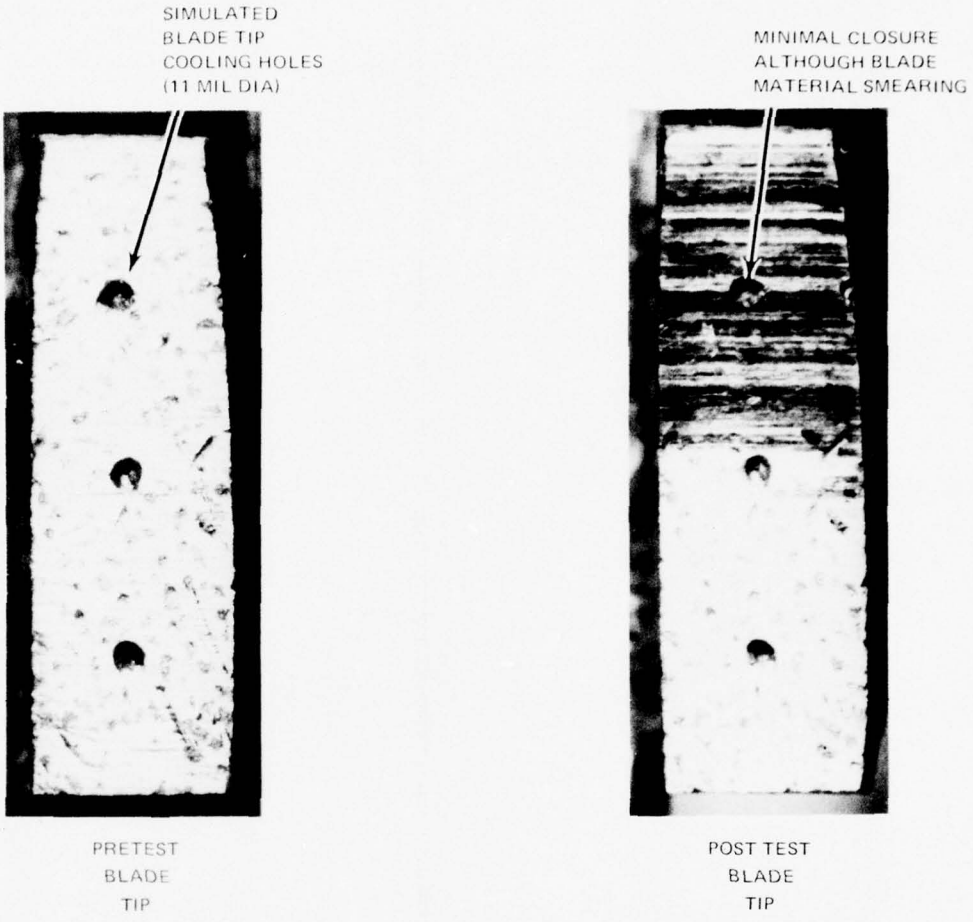

Figure 14 Rig Blades With Simulated Cooling Holes Showing Minimal Closure

GRADED ZrO_2-NiCr TURBINE SEAL

MATERIAL CHARACTERIZATION

The ZrO_2 layer of the graded ZrO_2-NiCr turbine seal system has been analyzed to determine its chemical, physical and mechanical properties and stability at high temperature. The effect of oxidation of the graded ZrO_2-NiCr intermediate layer was investigated.

A semi-quantitative spectroanalysis was performed on the zirconia region of the graded ZrO_2-NiCr seal system. The results show that Zr represents greater than 50% of the material, Ca 1-10% and Y 1-10%. The analysis also shows the presence of the impurity Si (0.5-5%), most probably present as SiO_2, in greater concentration than any other impurity element. All other impurities combined represent less than a total of 1%.

The zirconia layer was x-rayed for phase identification. The diffraction pattern confirmed that only cubic and monoclinic phases of zirconia were present in the ceramic region.

The bulk density of the zirconia region calculated directly by weight and dimensional measurements was very consistent with an average of 3.94 g/cm^3 and variation of ±0.002 g/cm^3. The measured true density was determined by a water displacement method to be 5.21 g/cm^3 and the theoretical density was determined by measuring the density of a sample of crushed powder from the zirconia region was 5.68 g/cm^3. The sample tested had 24.2% open cell porosity and 6.3% closed cell porosity.

The thermal conductivity of zirconia layer has been measured as a function of temperature, Figure 1. The zirconia is shown to be highly insulative and possesses, as expected, a lower thermal conductivity than the total structure thermal conductivity measured in Phase I.

The zirconia layer of the graded ZrO_2-NiCr system was tested in four point bending to determine modulus of elasticity and modulus of rupture of specimens "as fabricated" and after being aged for 10 hours at 3000°F. For the "as fabricated" specimens the modulus of elasticity was found to be 5.3 x 10^6 psi at room temperature and 0.12 x 10^6 psi at 2400°F. Modulus of rupture (MOR) was 3.5 x 10^3 psi at room temperature and 0.065 x 10^3 psi at 2400°F. The aged specimens exhibited reduced values of E and MOR which were 4.85 x 10^6 and 2.15 x 10^3 psi respectively. Metallographic analysis revealed that additional glassy phase, present in the "as fabricated" structure (Figure 2), formed and coalesced within the grain boundaries of the zirconia material during aging at 3000°F for 10 hours (Figure 3). The strength loss experienced by the aged specimens is a result of fracture propagating through the glassy phase and shrinkage cracks. Qualitative analysis of a microsection characterized the glassy phase as being Si-rich with lesser amounts of Ca and Al.

The kinetics of the reported coalescence and formation of glassy phase in the top layer zirconia grain boundaries was investigated. Samples of the top zirconia layer were isothermally aged in a high temperature air furnace, metallographically sectioned, and resultant grain growth was measured. Since grain growth is associated with the coalescence and formation of glassy phase in the grain boundaries, the change in grain size was used as a coincident indicator of glassy phase coalescence and formation. The results of these tests are summarized in Table I.

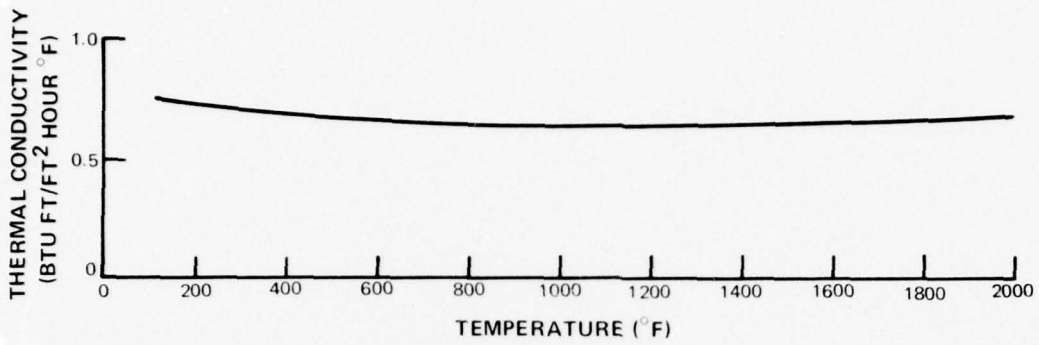

Figure 1 Thermal Conductivity of Graded ZrO_2-NiCr Seal System Zirconia Layer

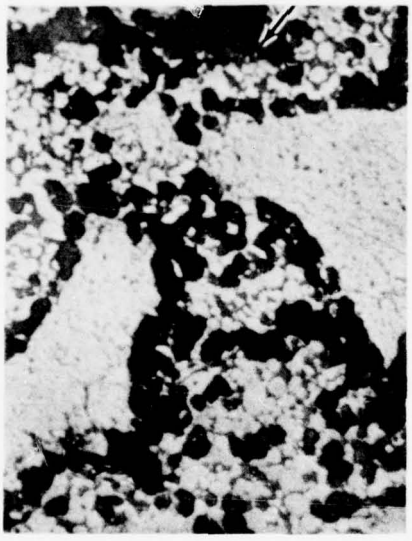

MAG: 750X

Figure 2 ***Microsection of As-Received Four-Point Bend Test Specimen Showing the Presence of a Glassy Phase Uniformly Distributed Throughout the Matrix Material (M74142)***

MAG: 200X

Figure 3 **SEM Photograph of Microsection of Aged Four-Point Bend Test Specimen**

TABLE I

MEASURED AVERAGE GRAIN SIZE OF ZIRCONIA AS A FUNCTION OF EXPOSURE TIME AND TEMPERATURE

	Time (Hours)					
Temperature (°F)	2	5	10	20	40	100
Room Temperature	7	7	7	7	7	7
2000	7	7	7	7	7	7
2500	– –	7	12	15	– –	– –
2850	– –	– –	– –	– –	36	– –
3000	15	20	37	– –	– –	– –

GRADED ZrO_2-NiCr TURBINE SEAL

MATERIAL CHARACTERIZATION (Cont'd)

The temperature dependence of the grain growth phenomenon was determined by construction of an Arrhenius plot of ln G/Go versus 1/T where Go is the starting grain size, G is the measured grain size after exposure and T is the temperature. Exposure time was held constant at 10 hours for this plot, Figure 4.

The time dependence of the grain growth phenomenon was determined by construction of a ln G versus ln t plot where t is exposure time in hours. The expected linear graphical relationships are observed at 3000°F and 2500°F, Figure 5. The one data point available at 2850°F was used to draw the expected linear behavior at this intermediate temperature level. The results show the dependence of grain growth with exposure time.

The Ni-Cr alloy used in the intermediate layer follows a normal parabolic oxidation behavior. Generally, uncoated porous NiCr structures are considered adequate for approximately 1200°F long term service (retains approximately 65% of original tensile strength after approximately 4000 hours). Glass coated porous NiCr structures are stable to 1600°F for long term service (retains approximately 65% of original tensile strength after approximately 3000 hours). The intermediate layer in the graded ZrO_2-NiCr seal system is composed of NiCr and ZrO_2 stabilized with Y_2O_3. The oxidation resistance of this composition is expected to be greater than the uncoated NiCr and less than the glass coated NiCr.

To evaluate the effect of oxidation of the intermediate layer on thermal fatigue capability, thermal fatigue specimens were oxidized at 1800°F for 100 hours and 1600°F for 100 hours prior to testing. The 1800°F sample was found to have fractured through the intermediate layer after the 100 hour exposure. The sample fracture is believed to have resulted from loss of intermediate layer strength due to oxidation of the NiCr in conjunction with creep of the NiCr at elevated temperatures and subsequent failure due to the stresses present in the "as-fabricated" sample. The 1600°F aged specimen survived 203 thermal fatigue cycles. Bend strength tests were conducted on "as-fabricated" and 1500°F/100 hr. aged specimens. The results of the tests are shown in Table II.

The microstructure of the aged specimens did not show any indication of oxidation or other structural changes compared to the unaged specimens. Failures in the aged specimens initiated at a known defect in the intermediate layer that was not present in the unaged specimen.

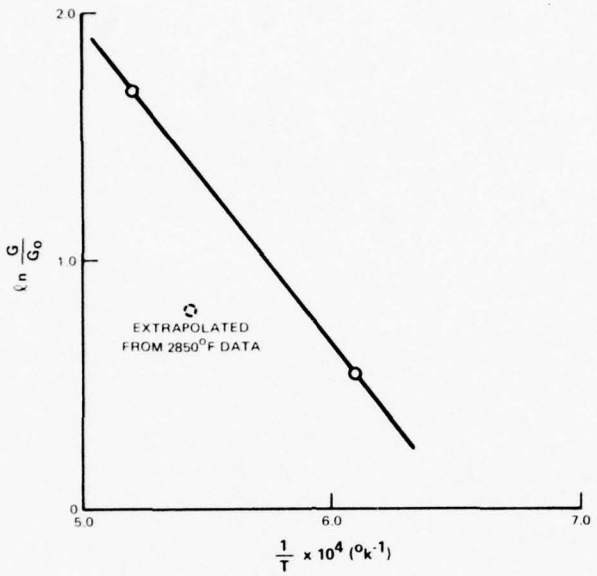

Figure 4 Arrhenius Plot of $\ell n \frac{G}{G_o}$ Versus 1/T for 10 Hour Exposures of the Top Zirconia Layer

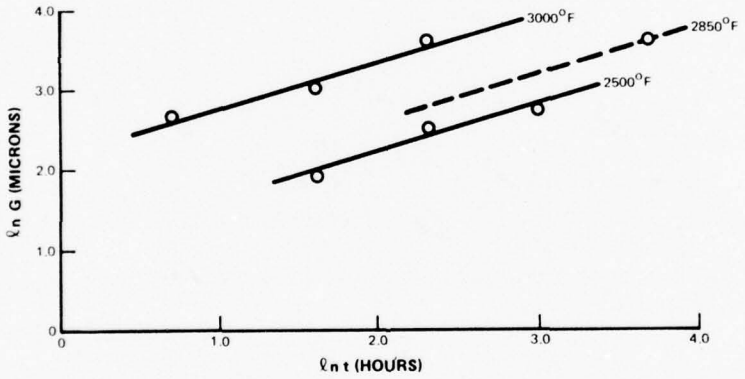

Figure 5 Plot of ℓn G Versus ℓn t for Exposure at Several Temperatures of the Top Zirconia Layer

TABLE II

BOND STRENGTH TEST RESULTS

Specimen	Bond Strength (psi)	Fracture Location
As-fabricated	470	Ceramic layer
1500°F/100 Hours	210	Intermediate layer-substrate interface and ceramic layer
1500°F/100 Hours	240	Ceramic layer-intermediate layer interface

GRADED ZrO_2-NiCr TURBINE SEAL

MATERIAL ANALYSIS TESTED RIG SPECIMENS

Post test material analysis of selected graded ZrO_2-NiCr turbine seal design thermal fatigue, erosion and rub rig specimens has been performed.

THERMAL FATIGUE SPECIMEN ANALYSIS

Microscopic examination of the "first" thermal fatigue specimen Number 1 tested "as-fabricated" verified the overtemperature test conditions that the specimen was subjected to. The degree of the ZrO_2 coalescence and shrinkage for 5 hours at maximum temperature was greater than exhibited by the 3000°F, 22 hour erosion specimen but less than the 3100°F, 22 hour erosion specimen. In addition the NiCr particles in the intermediate layer exhibited excessive oxidation which caused the bowing of the intermediate layer, which caused delamination at the intermediate-ceramic interface and in conjunction with the ZrO_2 shrinkage caused fracture of the ZrO_2 layer.

The excessive oxidation of the "as-fabricated", unaged specimen is characterized by a 0.2 to 0.5 mil oxide shell around the NiCr particles (Figure 1) as compared to less than 0.2 mil oxide thickness exhibited for the specimen preaged at 1800°F for 100 hours. The 1800°F, 100 hour specimen failure during aging is described in the Material Characterization section under oxidation discussion.

The 1600°F, 100 hour aged specimen survived 203 cycles. Microscopic examination of the specimen showed minimal oxidation of the NiCr particles and no significant adverse changes in the microstructure of the ZrO_2 layer due to coalescence. The specimen apparently failed due to fatigue type propagation of the cracks initiated during the aging process.

Metallographic analysis of "first modification" thermal fatigue specimen Number 2 was performed to determine the cause of cracks described in the Rig Specimen Testing section, page 17. Microscopic examination (Figure 2) of the sectioned seal revealed two major circumferential cracks within the intermediate layer starting at either end of the specimen extending diagonally upward toward the center of the specimen. These cracks are contained within the intermediate layer. The metal particles in the intermediate layers are oxidized above the circumferential cracks. Decreasing NiCr oxidation was observed from the ends of the specimen toward the center, in the region above the circumferential cracks. Oxidation of the NiCr metal particles also decreased from just below the ceramic layer toward the substrate but was negligible below the circumferential cracks. The distribution of NiCr oxidation indicates that the cracks were caused by thermal fatigue and that the oxidation occurred when locally high temperatures were produced above the cracks.

Figure 1 Thermal Shock Specimen Tested As-Built (M74164)

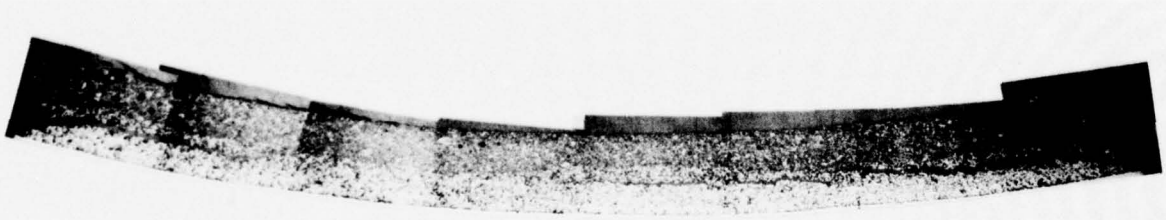

Figure 2 Metallographic Section of "First Modification" Thermal Fatigue Specimen No. 2

GRADED ZrO_2-NiCr TURBINE SEAL

MATERIAL ANALYSIS TESTED RIG SPECIMENS (Cont'd)

EROSION SPECIMEN ANALYSIS

Microscopic examination of the erosion specimens shows that the degree of coalescence of the Y_2O_3 stabilized ZrO_2 matrix particles and the degradation of the CaO stabilized ZrO_2 spheres progresses with exposure to increasing temperature (Figure 3). As is evident in the post test surface photographs, (Figure 4) the degree of the crack network within the ceramic structure progresses with increasing test temperature. This cracking in the ceramic layer is considered to be caused by a combination of the shrinkage due to sintering and coalescence; and creep and plastic flow of the ZrO_2 at maximum temperature conditions causing mud flat cracks when the specimens are returned to room temperature. The surface cracks observed in the erosion specimens normally arrested in the ZrO_2 layer as seen in the microsection of the specimen tested at 3100°F (Figure 5). It can be seen in Figure 6 that the surface crack networks are mainly encompassed in the ZrO_2 matrix and that the ZrO_2 spheres act as a crack arresting mechanism.

The SEM study indicates that the Y_2O_3 stabilized ZrO_2 matrix is primarily removed during high velocity erosion as seen in Figure 3 causing the weight loss detected.

Microscopic inspection of the erosion samples has verified that the quality from a thickness and uniformity standpoint of the "first" graded ZrO_2-NiCr seal design rig specimens was not of the desired level. Inadequacy in graduation of the intermediate layer probably caused the laminar cracks observed in the 3000°F and 3100°F erosion specimens. These cracks existed across approximately 70% of the intermediate layer. In addition the 3000°F specimen was found to have an area void of ZrO_2 spheres which probably allowed the surface cracks to propagate to the intermediate layer interface which caused delamination cracks across 35% of the specimen.

Examination of the "preliminary" seal design erosion specimens shows dramatic improvement in control of layer thickness during fabrication as evidenced by the NDI determination that the ZrO_2 layer average thickness variation is only ±4 mils. Control of graduation and homogeneity were satisfactory during fabrication of the "preliminary" specimens.

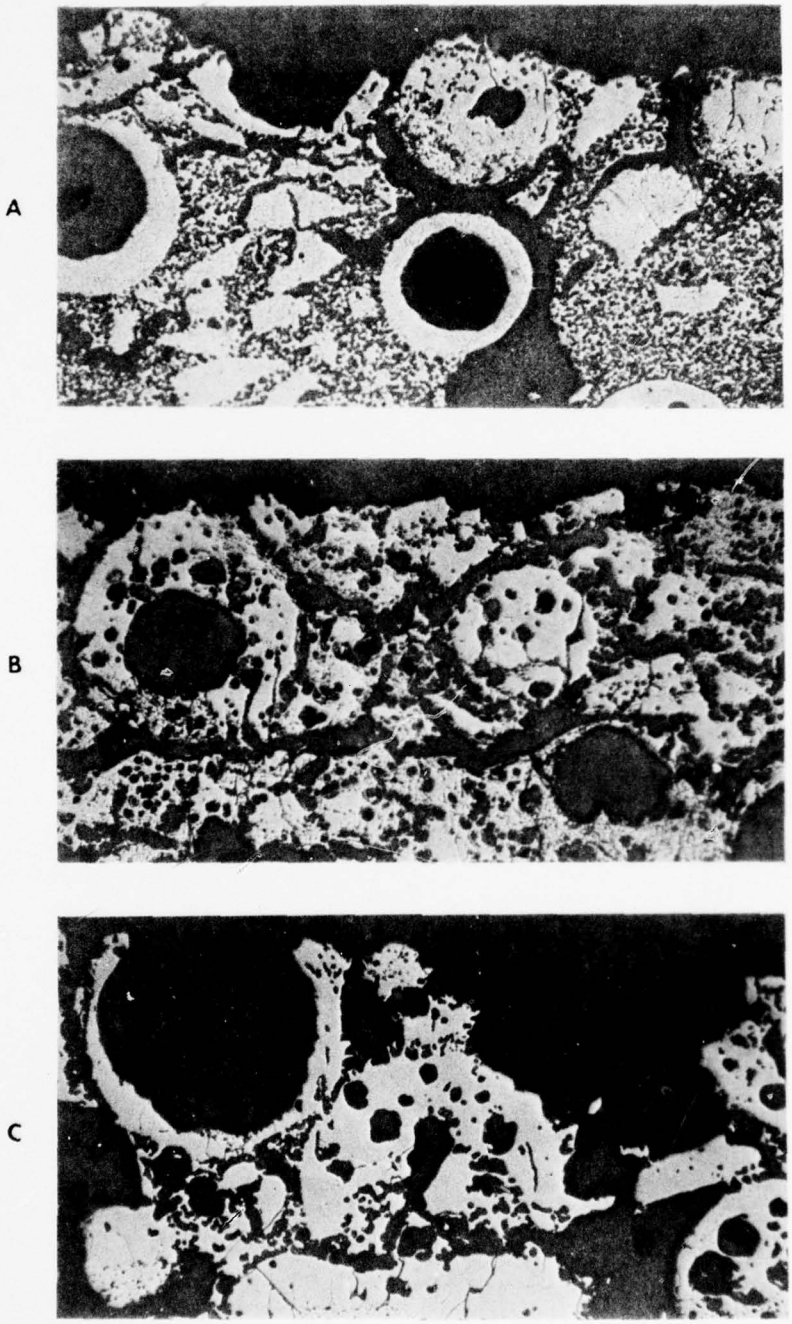

Figure 3 Microsections Near Surface of Post-Test Hot Gas Erosion Specimens: (A) 3000°F, (B) 3100°F, (C) 3200°F (M741383, M74182, M74181)

GRADED ZrO_2-NiCr TURBINE SEAL

MATERIAL ANALYSIS TESTED RIG SPECIMENS

EROSION SPECIMEN ANALYSIS (Cont'd)

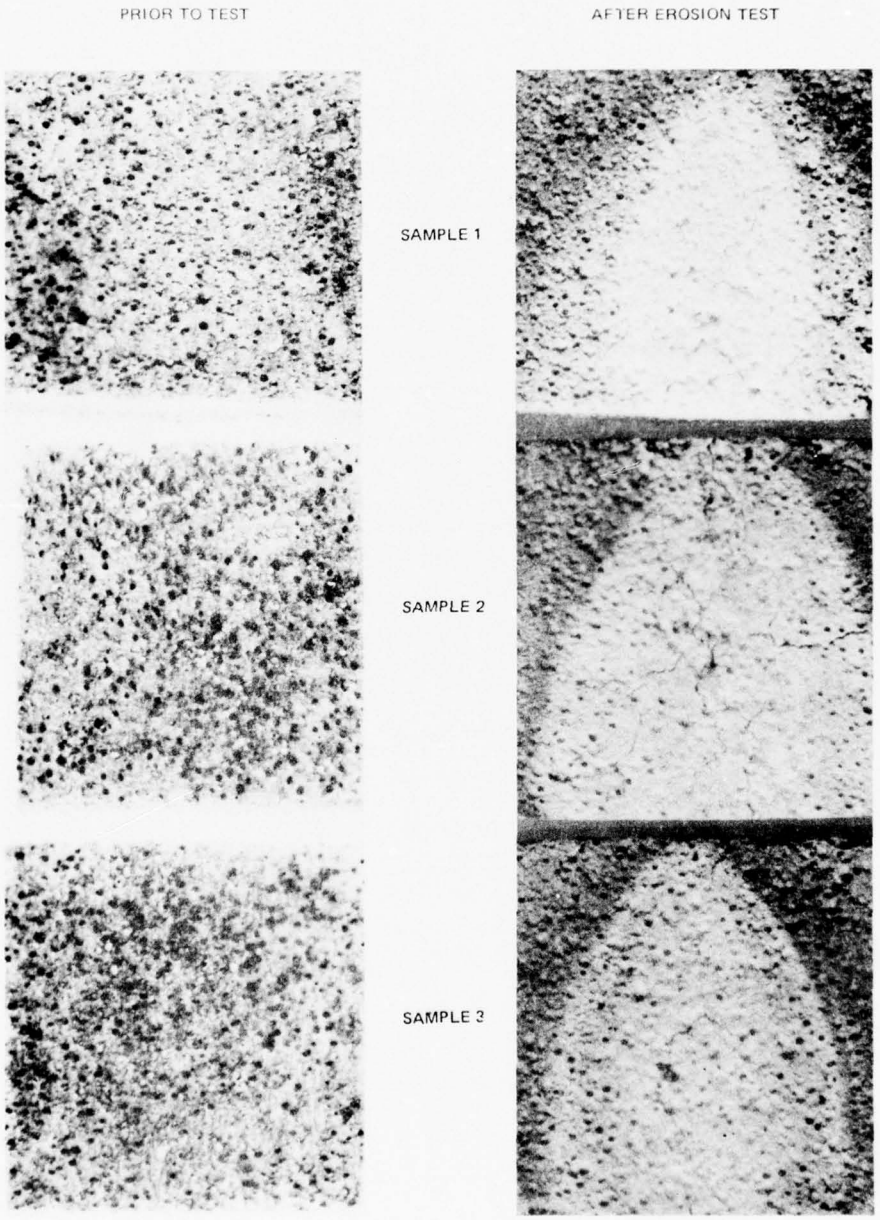

MAG: APPROX. 5X

Figure 4 "First" Graded ZrO_2-NiCr Erosion Test Specimens Before and After Test Exposure

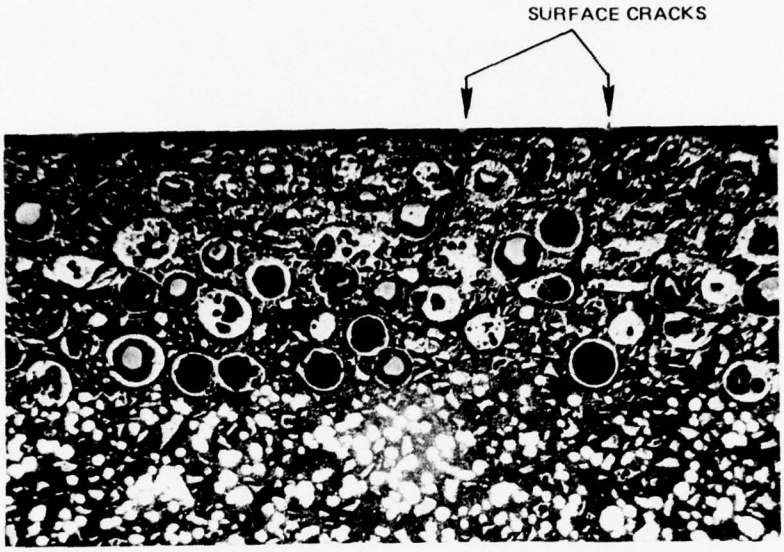

Figure 5 Cross Section of Hot Gas Erosion Specimen Showing Stable Mud Flat Cracks

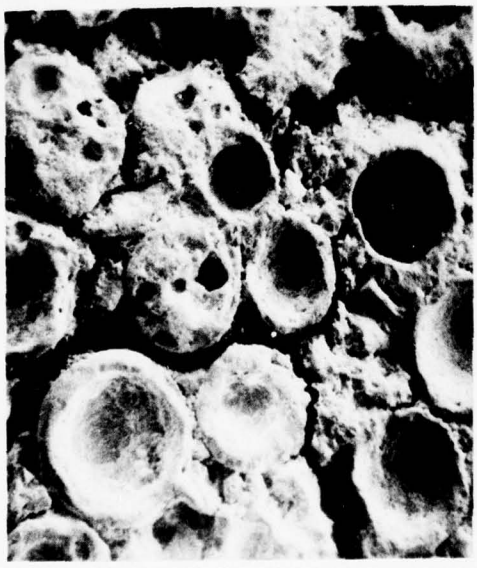

MAG: 60X

Figure 6 Surface of Specimen Erosion Tested at 3200°F

GRADED ZrO_2-NiCr TURBINE SEAL

MATERIAL CHARACTERIZATION (Cont'd)

RUB SPECIMEN ANALYSIS

Macroscopic examination of the "first" test phase rub specimen Number 2 showed the characteristic grooves induced by rub of the SiC abrasive grits against the seal structure. Specimen Number 1 experienced pull out of ZrO_2 matrix and spheres over approximately 10% of the rub path. Microscopic examination of this seal specimen (Figure 7) revealed large internal voids within the ceramic layer that apparently caused the pull out of surface material upon rub.

Slight transfer of nickel plate from the abrasive treated blade tips to the ZrO_2 surface of the room temperature rub specimens was observed macroscopically. The transfer of this nickel plate tended to initiate at ZrO_2 spheres that when probed were found to be either solid or thicker walled than normal.

Macroscopic examination of the "first" rub specimen number 3 run at 2500°F showed large areas of pull out in the rub path. Microscopic analysis of an unrubbed edge of this test specimen revealed sintering and melting of the ZrO_2 surface structure indicating temperatures in excess of 4000°F. The pull out observed in this specimen was a result of thermally induced cracking produced by the excessively high temperature experienced.

Microsection of the 2500°F rub specimen also revealed crack propagation characteristics similar to the erosion specimens where the cracks were redirected through matrix phase by the ZrO_2 spheres.

"Preliminary" rub specimen Number 3, tested at approximately 2700°F, and the SiC/M-CrAlY blade tip, which rubbed against it were analyzed. A section of the rubbed ZrO_2 seal was examined in the scanning electron microscope (SEM) and by standard metallographic techniques. The section analyzed in the SEM, Figure 8, showed typical rubbed and unrubbed areas. Within the rubbed area, a typical region indicated by A in Figure 8 was examined in greater detail, Figure 9. A generally smooth region with agglomerates on the surface was observed. These agglomerates were analyzed by dispersed x-ray analysis and was found to contain elements common to SiC, M-CrAlY and the zirconia seal material similar to Figure 10. Metallographic analysis performed on a typical cross-section of the rubbed specimen showed a relatively sharp groove in the ZrO_2 seal surface where the seal was rubbed, Figure 11. Microcracking of the ZrO_2 was observed along with particles of M-CrAlY (from the blade tip) below the rubbed surface. The presence of these M-CrAlY particles below the rubbed surface is an indicator of extremely high compressive stresses extruding metal from the blade tip into the porous zirconia seal material during the rub.

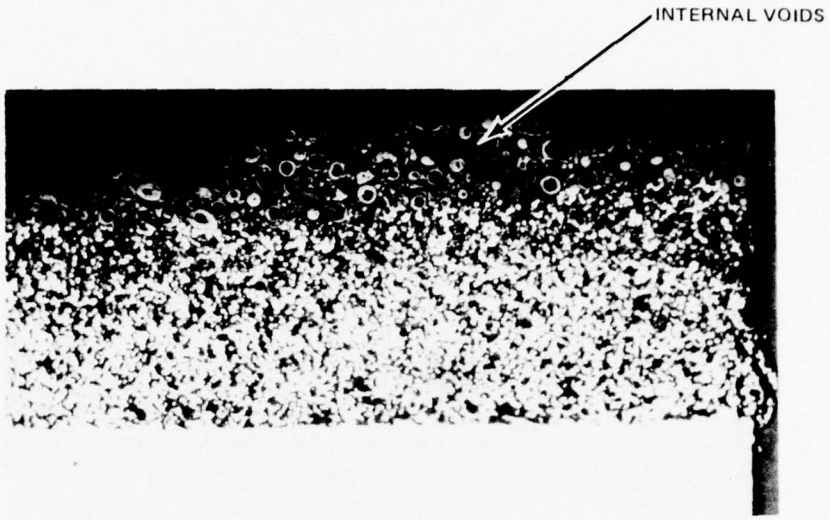

MAG: APPROX. 7X

Figure 7 Microsection of "First" Rub Specimen No. 1

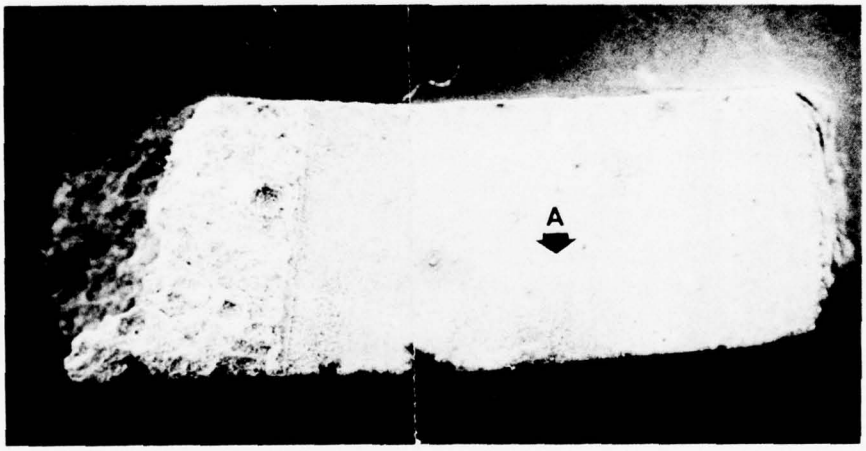

Figure 8 Section of Rub Tested Ceramic Seal Showing Rubbed and Unrubbed Areas. SEM Photograph at 19.6X

GRADED ZrO_2-NiCr TURBINE SEAL

MATERIAL CHARACTERIZATION

RUB SPECIMEN ANALYSIS (Cont'd)

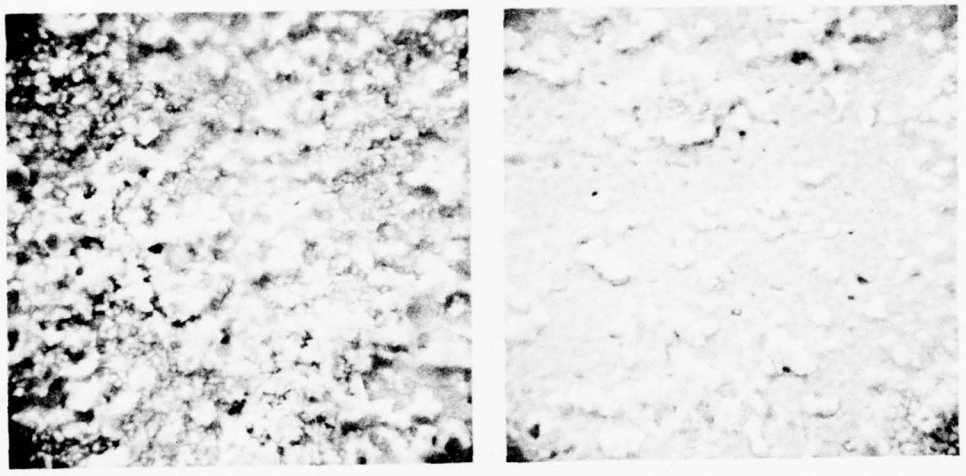

(a) (b)

Figure 9 Area A From Figure 14 at Tilt Angles of 90° (View a), and 20° (View b), Both at 2000X Magnification

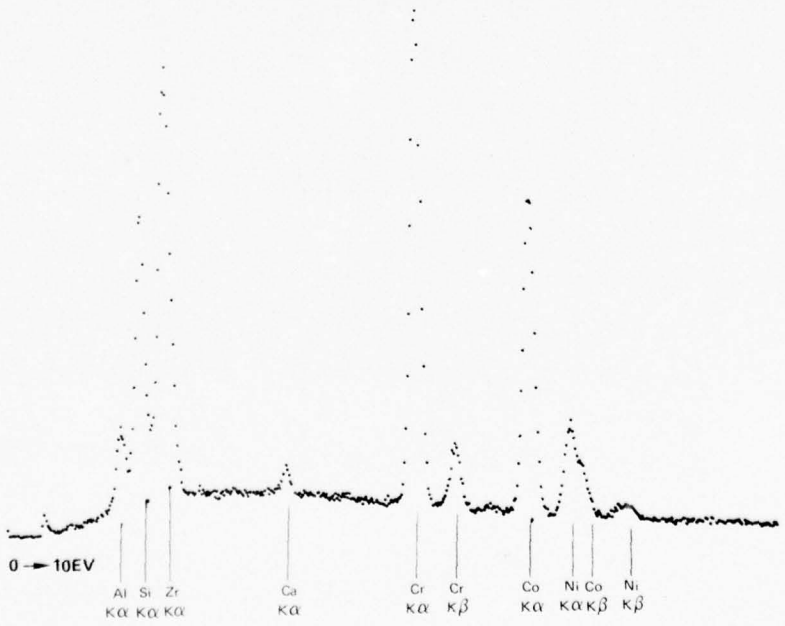

Figure 10 Dispersed X-ray Analysis of Typical Agglomerates

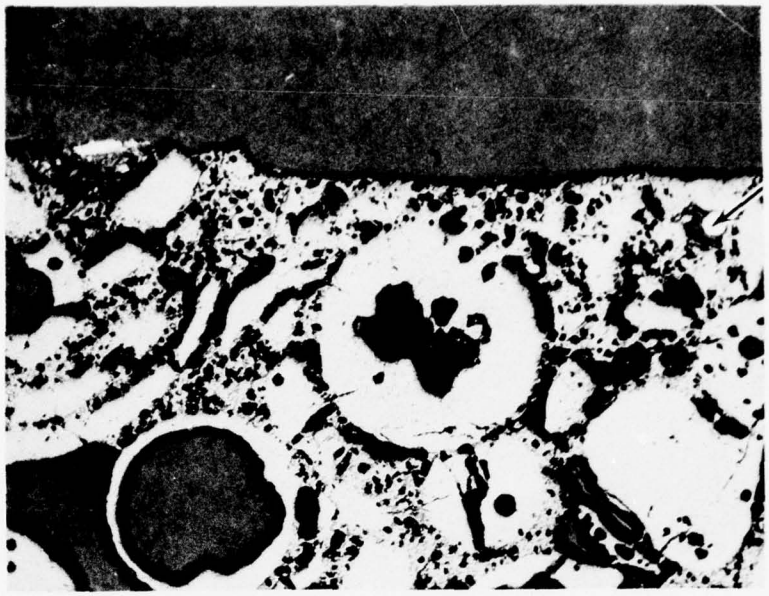

(a)

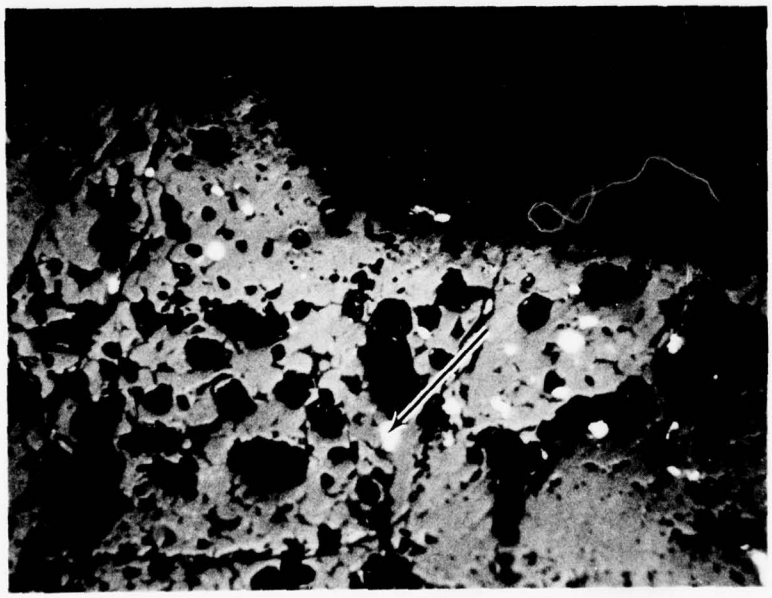

(b)

Figure 11 Typical Cross-Section Microstructure of Rub Tested Ceramic Seal Showing Relatively Sharp Groove As a Result of Rub Testing, and M-CrAlY Particles Below the Rubbed Surface. Magnification is 100X (View a), and 500X (View b)

K-16564

GRADED ZrO_2-NiCr TURBINE SEAL

MATERIAL CHARACTERIZATION

RUB SPECIMEN ANALYSIS (Cont'd)

The tested SiC/M-CrAlY blade tip is shown in Figure 12. The SiC particles can be clearly seen in the tip structure. Wear of the SiC particles produces smooth wear flats with some fracture observed, most probably as a result of pre-test machining damage. A typical SiC particle wear surface showing a smooth wear flat was examined as indicated in Figure 12. The surface of the SiC particle was observed to have a layer of smeared material unevenly deposited on the surface, Figure 13. Dispersed x-ray analysis was performed on areas 1 and 2 of Figure 13. Area 1 analysis, Figure 13 showed the presence of minor quantities of M-CrAlY elements. Area 2 analysis, Figure 13, showed the smeared material to be composed of elements common to both the M-CrAlY material and the zirconia seal material. A typical region of metal M-CrAlY matrix material was also examined in detail located in Figure 14. SEM examination of this area showed a severely deformed surface comprised of extruded metal smears in the rub direction. Dispersed x-ray analysis of a typical smear showed the presence of elements common to the M-CrAlY, SiC and zirconia seal system.

Based on the analysis of the rubbed M-CrAlY/SiC blade tip and zirconia seal material, the following wear mechanism can be deduced. Wear of the ceramic seal is believed to be primarily caused by abrasive wear of the SiC particles in the M-CrAlY metal matrix. During this wear process, M-CrAlY material is smeared over the SiC and zirconia rubbing surface. Extremely high compressive forces develop between the blade tip and seal material which causes extrusion of the M-CrAlY material into the porous zirconia seal material. Microcracking of the zirconia seal material also occurs as a result of these rubbing forces. Therefore, a combination of abrasive and adhesive mechanisms are believed active which produce smooth wear flats on the SiC particles and zirconia seal material.

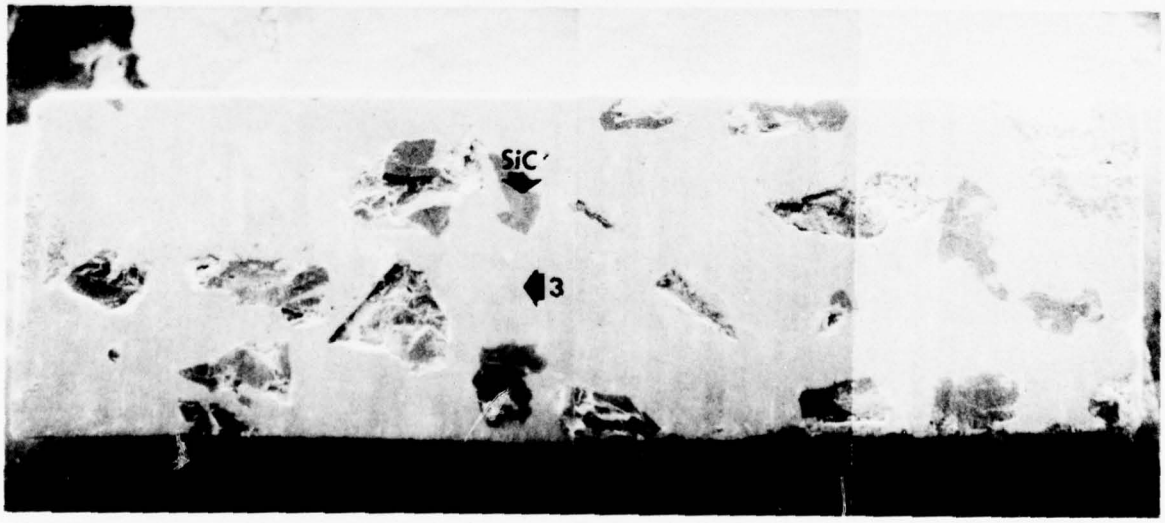

Figure 12 Rub Tested SiC/M-CrAlY Blade Tip. SEM Photograph at 18.7X

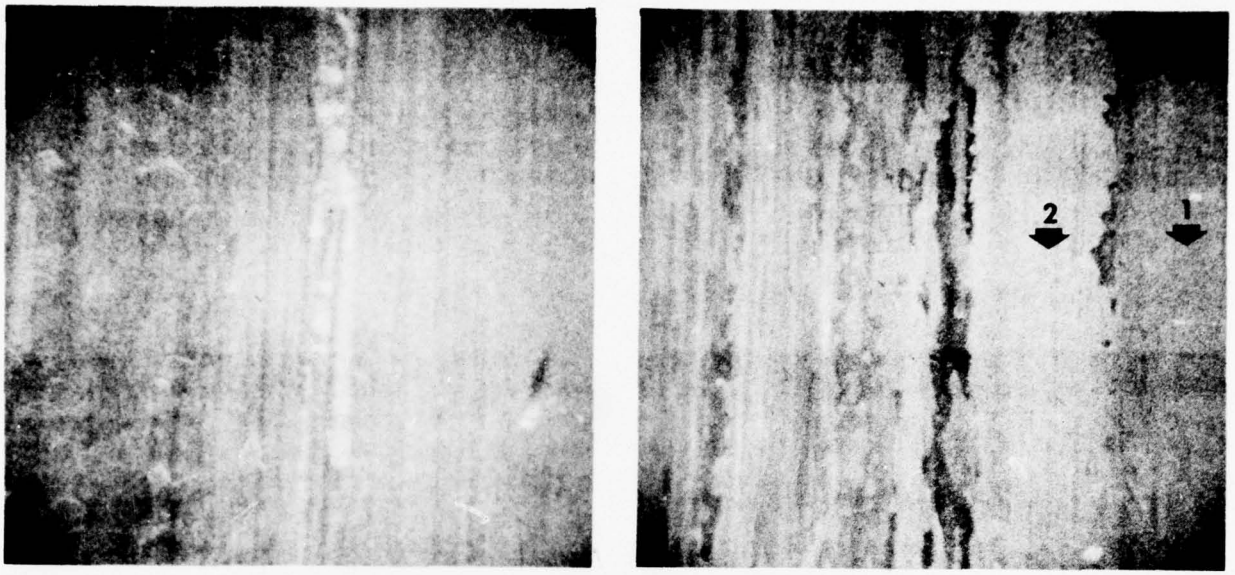

(a) (b)

Figure 13 SiC Particle Wear Surface Showing Smeared Material. SEM Photographs (View a and b) at 4700X. View a Tilt Angle – 90°, View b Tilt Angle – 20°

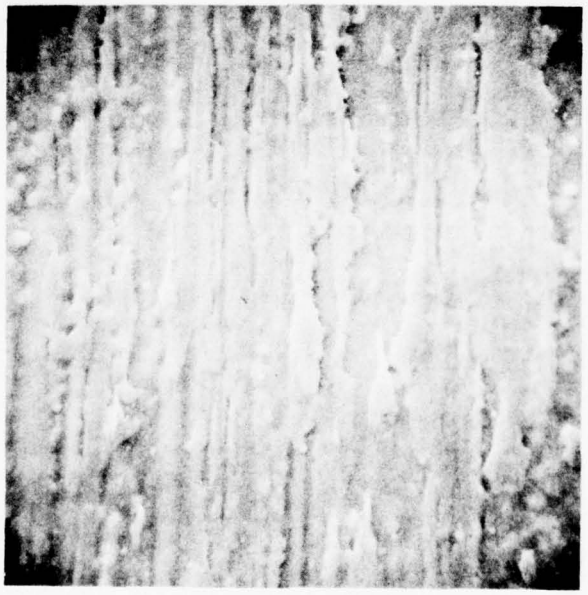

Figure 14 Typical Area of M-CrAlY Blade Tip Matrix. SEM Photograph at 1870X and 90° Tilt Angle

GRADED ZrO_2-NiCr TURBINE SEAL

NONDESTRUCTIVE INSPECTION

X-ray and ultrasonic inspection were shown to be effective nondestructive inspection (NDI) techniques for graded ZrO_2-NiCr seal hardware. Completed NDI of the "first modification" and "second modification" advanced engine ceramic seal rig specimens indicates a significant improvement in quality due to revised fabrication techniques.

RESULTS

The results of the nondestructive inspection (NDI) testing by x-ray and visual methods are summarized in Table I to Table V for all iterations of the graded ceramic-metal seal design rig specimens. With x-ray inspection it was possible to detect the depths of visual cracks (Figure 1, x-ray a), degree of thickness uniformity of the ZrO_2 layer (x-ray b), local density variation (x-ray c) and layer separation (x-ray d in Figure 1).

Visually observable surface cracks in some of the ZrO_2 layer of the specimen were shown to terminate in the graded ZrO_2-NiCr layer (Figure 1, x-ray a). These cracks were not considered to be critical.

TABLE I

SUMMARY OF NONDESTRUCTIVE INSPECTION RESULTS FOR "FIRST" ADVANCED ENGINE GRADED ZrO_2-NiCr SEAL SPECIMENS

Specimen	Visual Inspection (Surface Cracks)	X-ray Inspection			Ultrasonic Inspection Disbond Indication	
		Top Layer Uniformity (mils)	Layer Separation	Density Variation	Location	Amount (%)
Thermal Fatigue 1	None	70 ± 10	Edge	None	– – –	– – –
Thermal Fatigue 2	None	60 ± 10	Center[1]	None	None	None
Rub 1	One	65 ± 15	Edge	None	Edge	10
Rub 2	Three	75 ± 25	None	None	Edge, Center	15 – 20
Rub 3	One	60 ± 10	None	None	None	0
NDI Verification 1[2]	None	– – –	None	None	Edges	25 – 30
NDI Verification 2	None	70 ± 10	Edge[1]	None	Edges	25 – 30
NDI Verification 3	None	60 ± 10	Center[1]	One area[3]	None	None

1 Not certain
2 Fabricated nonuniform for NDI verification
3 Region of 0.15 inch diameter appeared less dense

TABLE II

SUMMARY OF NONDESTRUCTIVE INSPECTION RESULTS FOR "PRELIMINARY" ADVANCED ENGINE CERAMIC SEAL RIG SPECIMENS

Specimen	Visual Inspection (Surface Cracks)	X-Ray Inspection			
		Top Layer Uniformity (mils)	Layer Separation	Density Variation	Estimated Coating Thickness (inches)
Thermal Fatigue 1	None	– –	– –	– –	– –
Thermal Fatigue 2	None	100	Substrate	None	0.21
Thermal Fatigue 3	None	95 ± 5	None	Ceramic layer	0.22
Erosion 1	None	90	Slightly above substrate	None	0.22
Erosion 2	None	100	None	None	0.23
Erosion 3	None	100	Substrate	None	0.22
Rub 1	One Axial	– –	–	– –	– –
Rub 2	One Axial	90	Substrate	Intermediate layer	0.22
Rub 3	One Axial	– –	– –	– –	– –
NDI Verification 1	None	75 ± 5	Substrate	None	0.22
NDI Verification 2	None	95 ± 5	Substrate	Intermediate layer	0.22
NDI Verification 3	None	90	None	Intermediate layer	0.22
NDI Verification 4	One Axial	90 ± 10	Substrate	None	0.23

TABLE III

SUMMARY OF NONDESTRUCTIVE TEST RESULTS FOR THE "INITIAL" ADVANCED ENGINE CERAMIC SEAL RIG SPECIMENS

Specimen	Visual Inspection (Surface Cracks)*	X-Ray Inspection				Remarks
		Top Layer Uniformity (mils)	Layer Separation	Density Variation	Estimated Coating Thickness (in.)	
Thermal Fatigue 1	3	90 ± 10	None	Intermediate layer	0.18	
Thermal Fatigue 2	2	90 ± 10	None	Intermediate layer	0.17	
Thermal Fatigue 3	3	90	Top/intermediate interface	Intermediate layer	0.18	
Rub 1	2	55 ± 5	None	Two areas in intermediate layer	0.14	Excessive porosity at substrate interface
Rub 3	3	95 ± 25	Top/intertermediate interface	Intermediate layer	0.18	Porosity or crack indication observed; substrate separated
Rub 3	1	110	Intermediate layer	Intermediate layer	0.20	Circumferential cracking or porosity
Rub 4	1	90	Intermediate layer	Intermediate layer	0.20	Circumferential cracking or porosity

*All surface cracks are axial.

GRADED ZrO_2-NiCr TURBINE SEAL

NONDESTRUCTIVE INSPECTION

RESULTS (Cont'd)

TABLE IV

NON-DESTRUCTIVE INSPECTION RESULTS FOR THE "FIRST MODIFICATION" OF THE "INITIAL" ADVANCED ENGINE CERAMIC SEAL RIG SPECIMENS

		X-Ray Inspection				
Sample	Visual Inspection (Surface Cracks)	Top Layer Uniformity (mils)	Layer Separation	Density Variation	Estimated Coating Thickness (in.)	Remarks
Thermal Fatigue 1	0	88 ± 10	None	Intermediate layer	0.18	– –
Thermal Fatigue 2	0	88 ± 10	None	Intermediate layer	0.18	Possible bond problem
Thermal Fatigue 3	1	93	Intermediate layer	Intermediate layer	0.18	Laminar crack noted (0.5 inch length)
Erosion 1	2	125	None	Intermediate layer	0.21*	Top surface and edge irregularities
Erosion 2	2	93	None	Intermediate layer	0.20*	Top surface and edge irregularities
Erosion 3	3	109	None	Intermediate layer	0.20*	Top surface and edge irregularities
Rub 1	1	85 ± 8	None	Intermediate layer Top coat interface	0.17	– –
Rub 2	3	93	None	Intermediate layer	0.18	– –
Rub 3	0	93	None	Intermediate layer	0.18	Low density areas in two intermediate layers
Rub 4	1	85 ± 8	None	Intermediate layer	0.18	Some circumferential cracking, corner chip missing.

*Not machined using normal procedure.

TABLE V

NON-DESTRUCTIVE INSPECTION RESULTS FOR THE "SECOND MODIFICATION" OF THE "INITIAL" ADVANCED ENGINE CERAMIC SEAL RIG SPECIMENS

		X-Ray Inspection				
Sample	Visual Inspection (Surface Cracks)	Top Layer Uniformity (mils)	Layer Separation	Density Variation	Estimated Coating Thickness (in.)	Remarks
Thermal Fatigue 1	2	100 ± 5	None	Intermediate layer	0.20	– –
Thermal Fatigue 2	1	103 ± 3	None	Intermediate layer (½ circumference)	0.20	– –
Thermal Fatigue 3	3	98 ± 5	None	None	0.19	– –
Erosion 1	1	103 ± 3	Slight separation in intermediate layer	None	0.20	– –
Erosion 2	0	– –	– –	– –	– –	No x-ray available
Erosion 3	1	– –	– –	– –	– –	No x-ray available
Rub 1	1	95 ± 5	Intermediate layer	None	0.18	Slight laminar crack in center of segment
Rub 2	3	105 ± 5	None	None	0.20	
Rub 3	4	98 ± 5	None	Intermediate layer (½ circumference)	0.19	
Rub 4	2	100 ± 8	None	Intermediate layer	0.20	

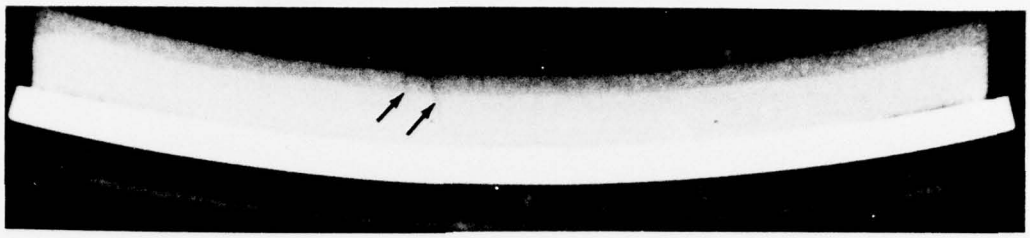

a. CRACKS

b. DEGREE OF THICKNESS UNIFORMITY

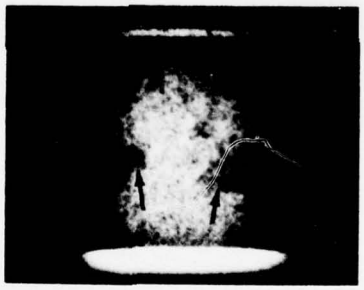

c. LOCAL DENSITY

d. LAYER SEPARATION

Figure 1 Examples of X-Ray Detection Capability on Seal Test Specimens

GRADED ZrO_2-NiCr TURBINE SEAL

NONDESTRUCTIVE INSPECTION

RESULTS (Cont'd)

A 1-million-volt x-ray can determine thickness variations of ±10 mils in the layers of the graded ZrO_2-NiCr seal system. The ZrO_2-NiCr thickness of the "first" seal specimens (Table I) had an average deviation of ±13 mils. The average deviation of the seal specimen thickness variation for the remaining test iterations was lower ("preliminary" ±3, "initial" ±7, "first modification" ±4, and "second modification" ±4) as a result of improved control of processing parameters.

Local density variations were observed (Figure 1, x-ray c). Areas of lesser density appear slightly darker than adjacent regions in the figure. When this specimen was later sectioned, one of the density variations was found to be associated with a void at the substrate interface and with some porosity within the ZrO_2 layer.

Ultrasonic inspection of the samples was also performed on "first" advanced engine specimens to determine nonbonded regions in the samples for the purpose of detecting bond inadequacy at the braze joint. The results of the ultrasonic inspection are also summarized in Table I. A map of each sample (Figure 2) shows the indicated areas of disbond as shaded areas. In general, the disbond areas are associated with the axial (short) edges of the specimens.

The hardness of the zirconia surface was measured on a superficial Rockwell hardness tester using a 45 Kg load and a ½" diameter ball (Y) indenter. The hardness data shows the improvement in quality of specimens due to revision of mixing, forming and bonding techniques after fabrication of the "initial" specimens as discussed in the Fabrication Quality Control section on page 15. The average hardness of the "initial" (Table VI) specimens was 59. The improved "first modification" (Table VII), and "second modification" (Table VIII) specimens had average hardnesses of 67 and 69, respectively.

For engine quality hardware, Pratt & Whitney Aircraft recommends the following nondestructive inspection goals:

A. Visual (up to 60X magnification)
   1. No circumferential or axial cracks.

B. Hardness (Rockwell 45Y)
   1. Hardness Range 65-75.
   2. Minimum-maximum hardness range of 15 on each specimen.

C. X-Ray (1 million volt)
   1. No circumferential and axial laminar cracks.
   2. Minimum density variation regions located in low stress location.

D. Thickness (Micrometer and X-Ray)
   1. ± 0.008 inches of total designed thickness.
   2. Intermediate layer thickness of ± 0.002 inches.

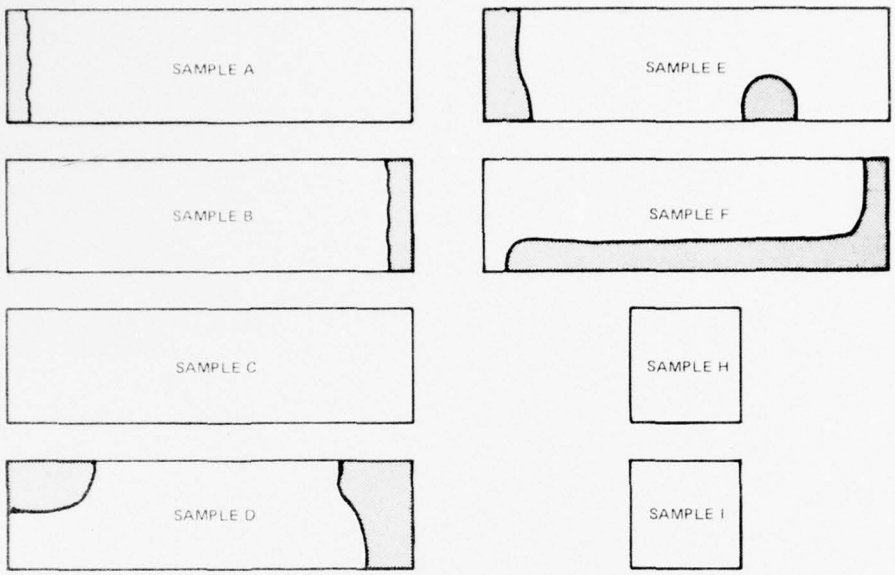

Figure 2 Ultrasonic Indications of Disbond (Shaded Regions) on Seal Test Specimens

TABLE VI

SUMMARY OF HARDNESS DATA FOR THE "INITIAL" ADVANCED ENGINE CERAMIC SEAL RIG SPECIMENS

Specimen	Hardness Range (Rs45Y)	Hardness Average (Rs45Y)
Thermal Fatigue 1	25 - 80	61
Thermal Fatigue 2	49 - 82	69
Thermal Fatigue 3	40 - 68	56
Erosion 1	37 - 63	50
Erosion 2	55 - 58	57
Erosion 3	68 - 73	71
Rub 1	54 - 83	67
Rub 2	54 - 70	62
Rub 3	40 - 54	47
Rub 4	30 - 72	56

TABLE VII

HARDNESS DATA FOR THE "FIRST MODIFICATION" OF THE "INITIAL" ADVANCED ENGINE CERAMIC SEAL RIG SPECIMENS

Specimen	Hardness Range (Rs45Y)	Average Hardness (Rs45Y)
Thermal Fatigue 1	61 - 71	67
Thermal Fatigue 2	56 - 78	69
Thermal Fatigue 3	47 - 77	61
Erosion 1	53 - 63	58
Erosion 2	63 - 78	71
Erosion 3	53 - 72	64
Rub 1	62 - 75	69
Rub 2	61 - 76	69
Rub 3	67 - 80	72
Rub 4	60 - 72	65

TABLE VIII

HARDNESS DATA FOR THE "SECOND MODIFICATION" OF THE "INITIAL" ADVANCED ENGINE CERAMIC SEAL RIG SPECIMENS

Specimen	Hardness Range (Rs45Y)	Average Hardness (Rs45Y)
Thermal Fatigue 1	62 - 87	73
Thermal Fatigue 2	53 - 82	69
Thermal Fatigue 3	54 - 79	68
Erosion 1	30 - 65	53
Erosion 2	66 - 85	73
Erosion 3	55 - 70	63
Rub 1	65 - 85	73
Rub 2	58 - 82	72
Rub 3	52 - 71	65
Rub 4	57 - 85	75

GRADED ZrO_2-NiCr TURBINE SEAL

NONDESTRUCTIVE INSPECTION (Cont'd)

METALLURGICAL VERIFICATION

Metallurgical verification was conducted on a specially fabricated nondestructive inspection (NDI) specimen (Figure 3, sample 1) and two test specimens (Figure 3, samples 2 and 3). The dotted lines indicate the planes that were examined metallurgically, the shaded areas in samples 1 and 2 are the areas of disbond determined ultrasonically, and the crosshatched areas in sample 3 are the density variations from x-ray. The plane 1a, which is the 20- to 90-mil ZrO_2 layer that had been specially prepared for NDI, is shown metallurgically in Figure 4. Microstructure at plane 1b is shown in Figure 5.

Specimen 2 was sectioned in two areas to verify the ultrasonic disbond indications. Metallurgical examination at planes 2a and 2b clearly showed that the ultrasonic indications are associated with a separation between the graded ceramic-metal system and MAR-M-509 substrate (Figure 6).

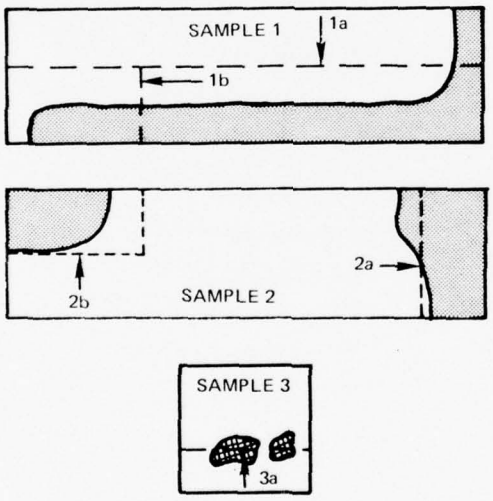

Figure 3 Locations of Metallurgical Sections Taken on Seal Test Specimens

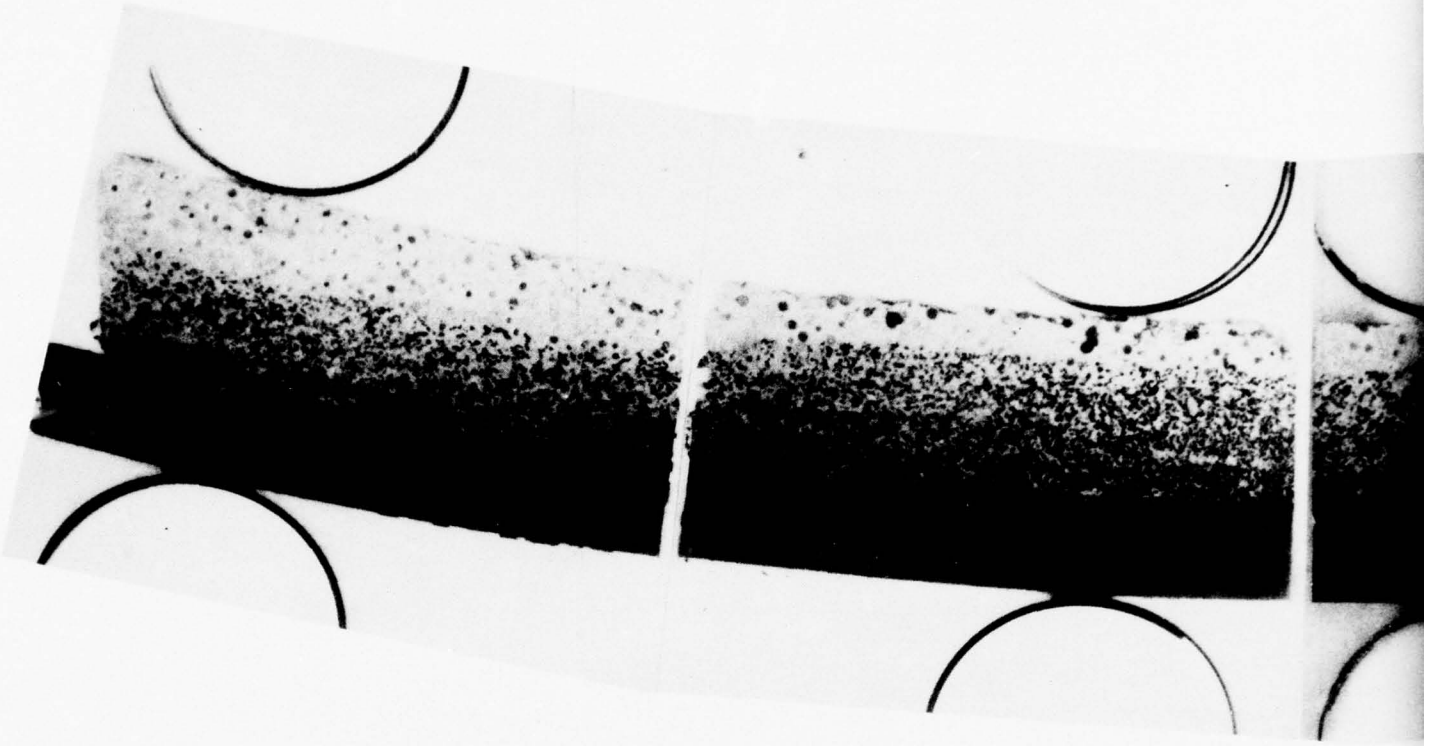

Figure 4 Metallographic Section at Plane 1a in Seal Sample 1 Showing the 20- to 90-Mil Zr

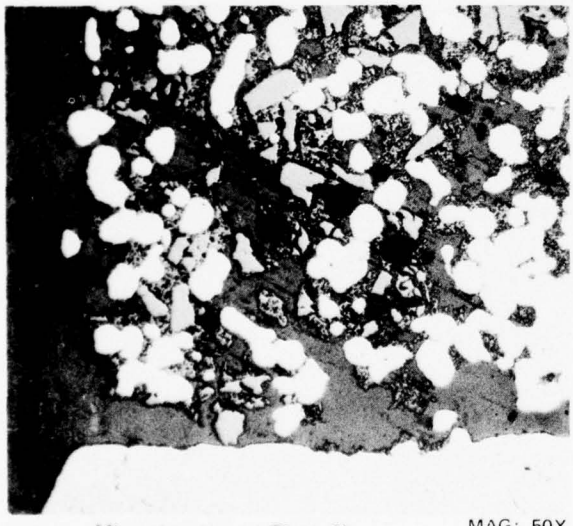

MAG: 50X

Figure 5 Microstructure at Plane 1b in Seal Sample 1, Verifying the Ultrasonic Inspection Indications of Disbond at the Interface of the Graded ZrO_2-NiCr Layer and the Substrate

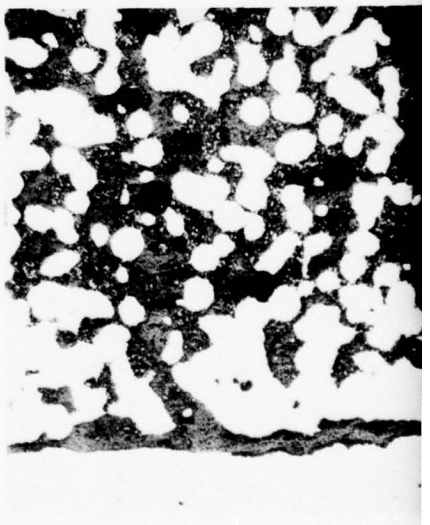

Figure 6 Microstructu
Indications

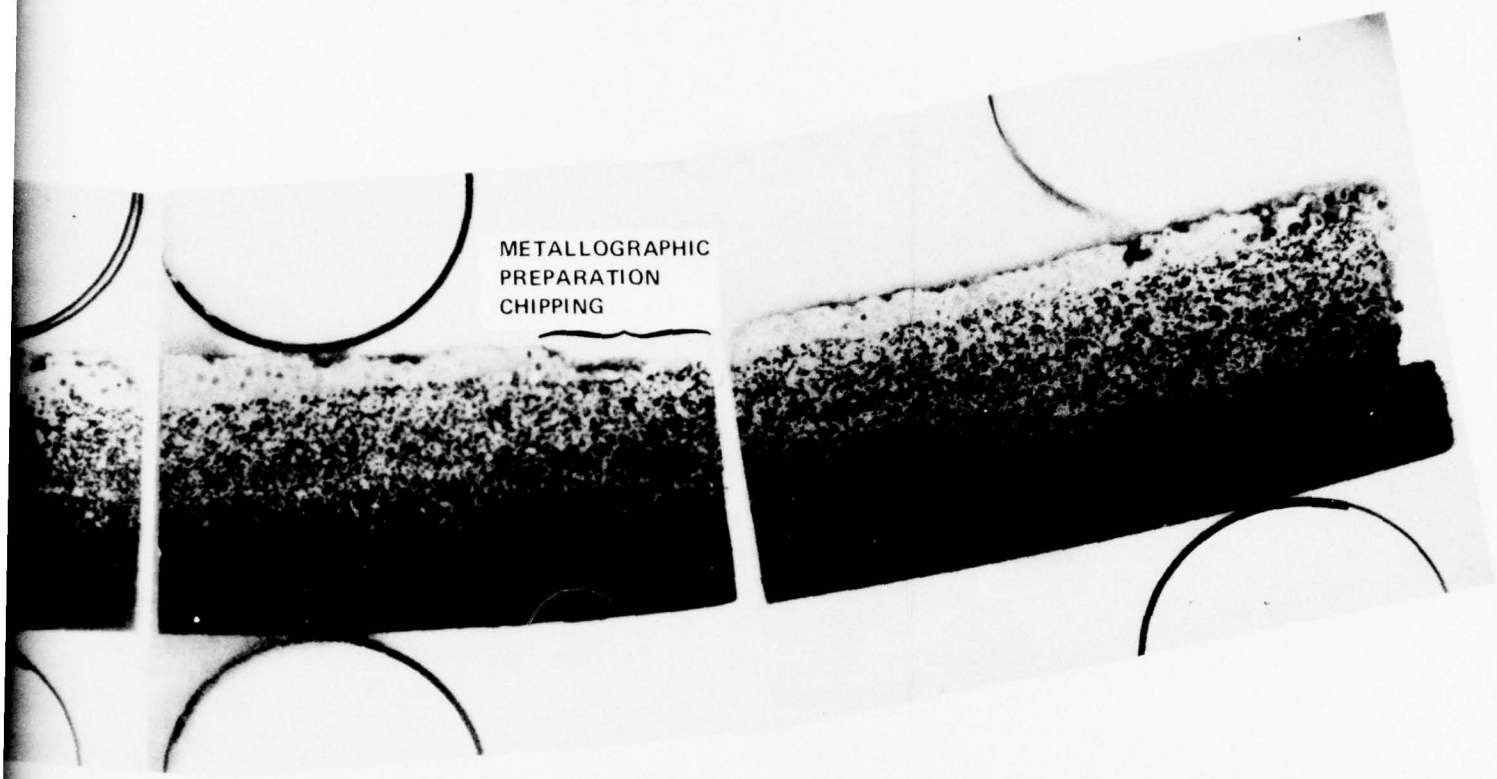

owing the 20- to 90-Mil ZrO_2 Layer Specially Prepared for Ultrasonic Nondestructive Inspection

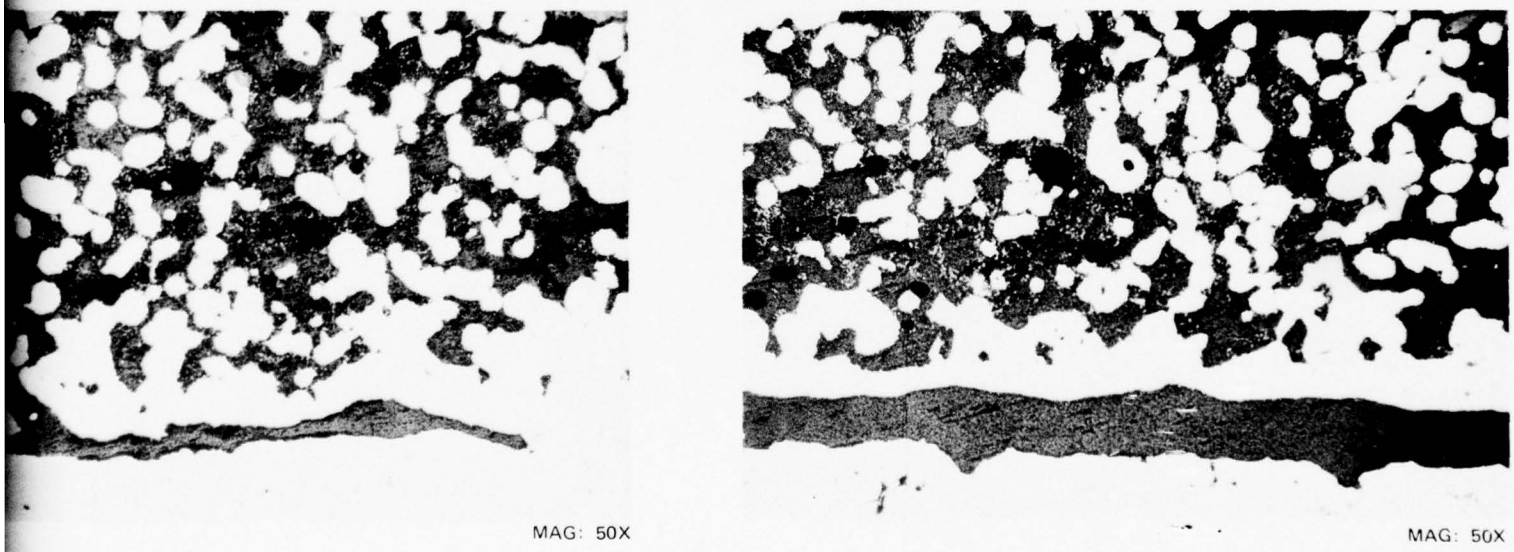

Figure 6 Microstructure at Planes 2a (Right) and 2b (Left) in Seal Sample D, Verifying the Ultrasonic Inspection Indications of Disbond at the Interface of the Graded ZrO_2-NiCr Layer and the Substrate

GRADED ZrO_2-NiCr TURBINE SEAL

NONDESTRUCTIVE INSPECTION

METALLURGICAL VERIFICATION (Cont'd)

Specimen 3 was examined to characterize the density variations shown by x-ray. The metallographic section (Figure 7) shows a void near the metal substrate approximately 0.140 inch long. A low density area in the ZrO_2 layer is located almost directly above the void.

It is concluded from the results of the metallurgical examination of specimen 3 that x-ray techniques will be able to distinguish three types of defects not observable by visual inspection: (1) nonuniformity of ZrO_2 layer thickness, (2) separation of the graded ceramic-metal system from the substrate, and (3) porosity within the graded ceramic-metal system. It is also concluded that ultrasonic inspection is capable of distinguishing unbonded regions of the specimens which x-ray may not indicate because of lack of sufficient separation between the graded ceramic-metal system and the metal substrate.

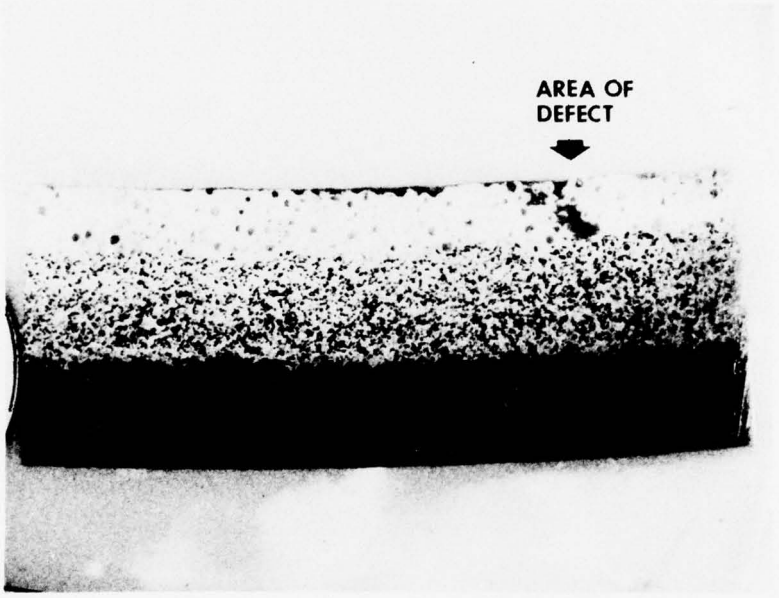

MAG: 5X

Figure 7 Metallographic Section at Plane 3a in Seal Sample 3 Showing Density Variations in the Graded ZrO_2-NiCr Layers; Variations Had Been Detected by X-Ray

STRUCTURAL CERAMIC TURBINE SEAL

DESIGN

The "first" and only structural ceramic advanced engine turbine seal mechanical design utilizing silicon carbide emphasized minimum complexity and cooling air requirements.

The major design considerations are similar to the graded ceramic-metal seal design, except that the silicon carbide (SiC) seal design does not have a "built-in" compliant method of attachment to metal. The SiC-metal attachment design must have high compliance and intimate bearing surfaces to insure nonlocalized load transfer from SiC to metal. The SiC design considers local strain conditions, not average strain as is the case for metals; therefore, sharp corners, small tabs, and other stress concentrations were avoided. The SiC material was treated as a brittle material, and its ductile behavior at high temperature was disregarded.

Impingement cooling was selected for its design flexibility and high cooling effectiveness. Flexibility to tailor the cooling by adjusting the impingement plate hole size, spacing, and distance from the SiC backside surface was a significant consideration.

Minimum leakage radially and axially is another important consideration. Radial leakage refers to the loss of cooling air into the main gaspath, and axial leakage refers to the main gaspath air that bypasses turbine blades and flows between SiC ceramic tiles. Analysis of engine running gaps between SiC ceramic tiles determined that the gap was only 0.0025 inch. The axial leakage was therefore considered to be minor. Radial seals are required and, as in the case of the attachment design requirement, should be highly compliant at the SiC-metal interface.

The turbine structural ceramic seal design that evolved is shown in Figure 1. This design incorporates a compliant attachment that is positioned out of the main gaspath at a predicted temperature level that is desirable from a structural and corrosion standpoint. The design incorporates a compliant radial seal that also restrains the SiC tiles circumferentially by pinning alternate radial seals (Figure 1). SiC tiles are presently attached to four metal segments that are conventionally attached to the case, thus reducing overall complexity.

The SiC seal design is compatible with the P&WA advanced engine except that it requires replacement of the seal supports and the 1st vane attachment to accommodate the cross-sectional thickness requirement of the SiC.

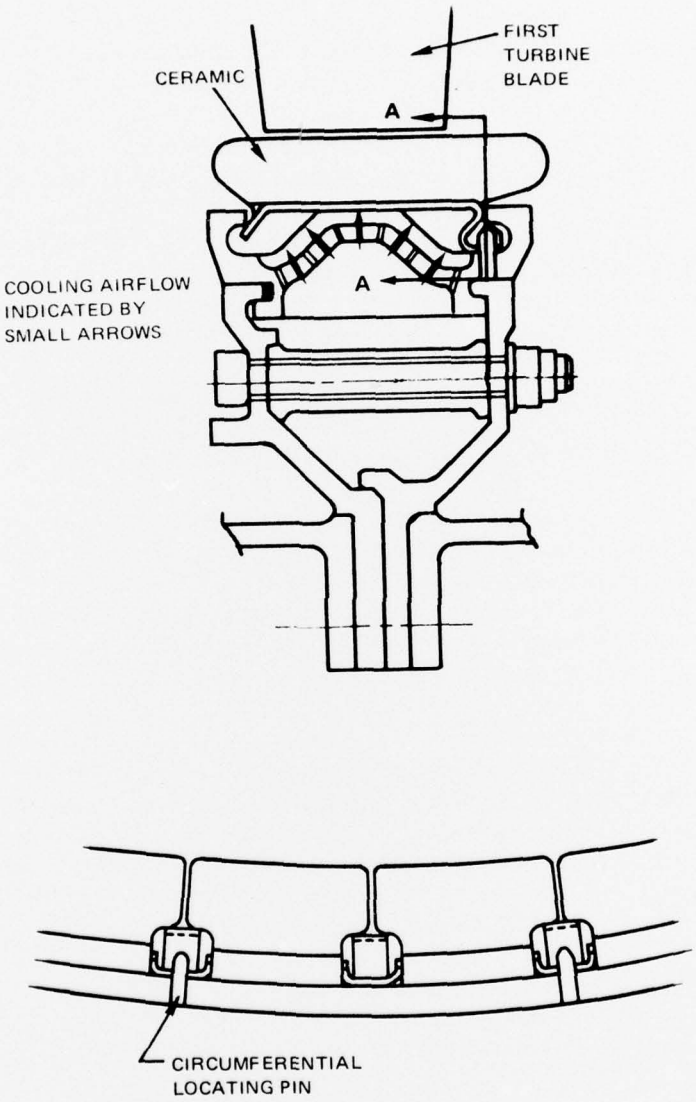

Figure 1 Cross Section of "First" Structural Ceramic Turbine Seal

STRUCTURAL CERAMIC TURBINE SEAL (Cont'd)

THERMAL AND STRUCTURAL ANALYSIS

Thermal and structural analysis of the "first" structural ceramic turbine seal design indicated acceptable stress levels but unacceptable distortion.

Thermal analysis of the silicon carbide structural ceramic seal design was conducted with the same two-dimensional finite-difference computer program as used for the graded ceramic-metal seal analysis. While the high temperature capability and thermal conductivity of silicon carbide made possible the cooling of the seal with only 0.3% W_{ae}, a fine line was encountered between overcooling the ceramic tabs in the attachment region with attendant thermal stress problems and excessive temperature in the metal hooks used to grip the silicon carbide tiles. Although several possibilities were considered to make the attachment compliant, the only viable method devised was to allow the MAR-M-509 support member to operate near its maximum temperature in the contact region. As shown in the results of the thermal analysis at hot spot full power conditions (Figure 1) the metal support contact points with the ceramic tile are approximately 1800°F. The maximum silicon carbide temperature is below its design limit.

Two-dimensional finite-element structural analysis was used to determine stresses that are thermally induced. Structural analysis utilizes approximately 2.5 times the number of finite elements as the thermal analysis. The more stringent analysis is required because of the criticality of local stress distributions which are geometry oriented. As shown in Figure 2, the stresses in the ceramic are low, less than 50 percent of the allowable working stress throughout. The maximum stress in the ceramic is in the radius near the rear attachment. The stresses calculated for the metal tile support are much closer to the design limits (75 percent). In the high temperature region near the tile support tabs, some yielding of the metal in compression is predicted but will not affect the life of the part.

The principal difficulty encountered in the structural ceramic seal analysis is in the area of distortion and leakage. The thermal gradient in the metal at the SiC-metal attachment location is 300°F per inch. The circumferential stress of the quarter-segment design proposed was found to give an unacceptable radial distortion of approximately 150 mils. To reduce the distortion to an acceptable level would require increasing the number of segments, which would increase the potential leakage.

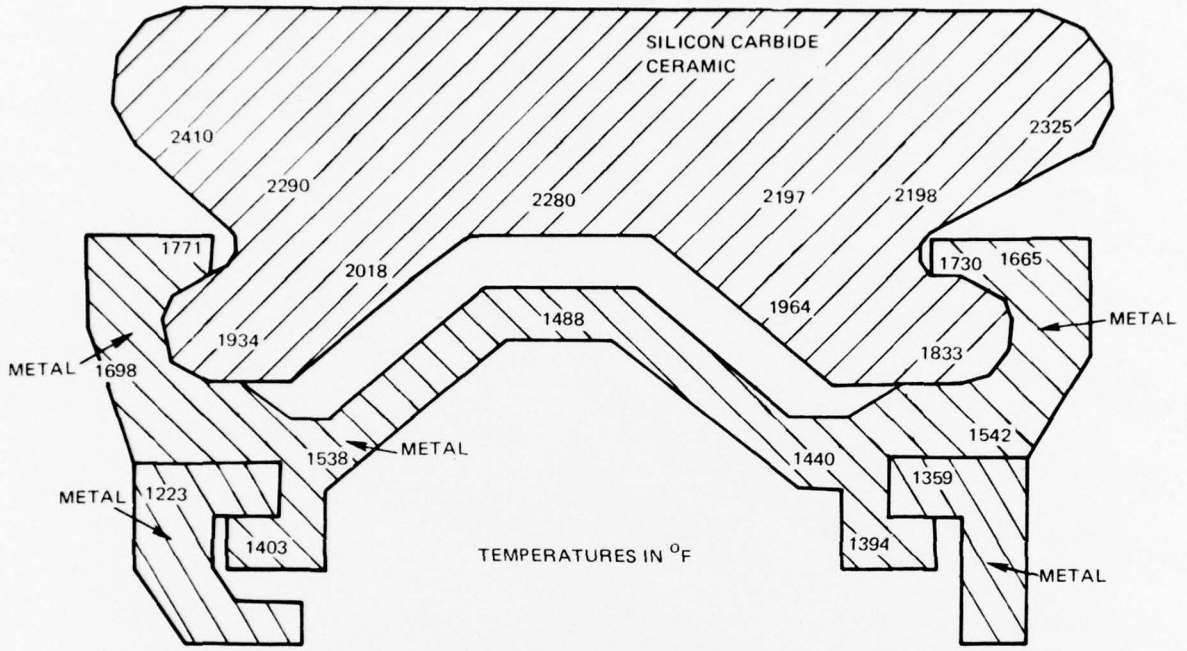

Figure 1 Thermal Map of "First" Advanced Engine Structural Ceramic Turbine Seal Design

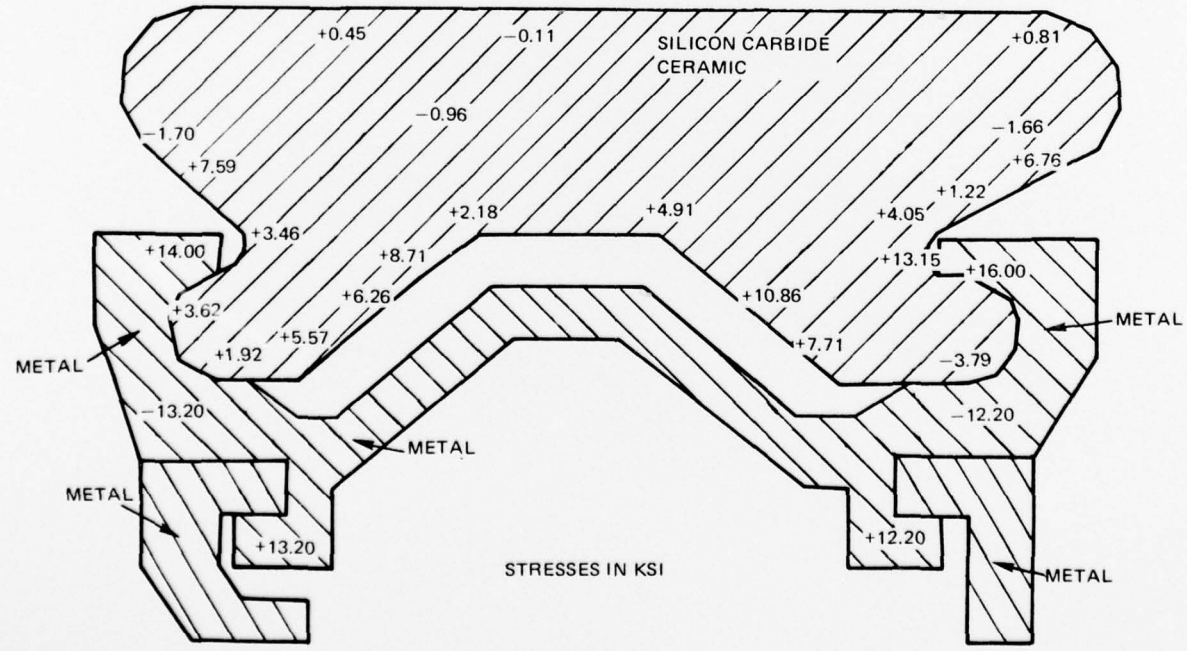

Figure 2 Stress Map of "First" Advanced Engine Structural Ceramic Turbine Seal Design

STRUCTURAL CERAMIC TURBINE SEAL (Cont'd)

RIG SPECIMEN TESTING AND ANALYSIS

Fabrication and testing of the rub and erosion specimens was completed. Thermal fatigue specimen fabrication was terminated upon receiving NAPTC concurrence with P&WA's recommendation to proceed with the graded ZrO_2-NiCr seal design only.

Design of the specimens for rub, erosion, and thermal fatigue rig testing the structural ceramic seal concept has been completed. The rig specimen design is based on the "first" advanced engine structural ceramic turbine seal design.

Hot gas erosion specimens (Figure 1) simulate engine seal cross-sectional construction, but not the shape or retention method since the basic intent is to determine experimentally the surface durability, or life at engine predicted surface temperatures. The final design of the rub test specimens (Figure 2) was chosen to minimize procurement time. P&WA rub test experience has shown that accurate data can be obtained from this simple design.

Thermal fatigue specimen design is the same (Figure 3) as a full-size ceramic tile supported in a manner similar to that used in the engine seal design. Procurement of the specimens was terminated at the time NAPTC approved the P&WA recommendation to proceed with the graded ZrO_2-NiCr seal design.

Hot gas erosion tests at 2600°F, 2700°F and 2800°F, and Mach 0.8 gas velocity were completed with a predicted erosion life of 7300, 6860 and 6250 hours to 10 mils, respectively.

One specimen of each of the two rub test configurations (Figure 1) was rubbed with test blades tipped with silicon carbide abrasive grits encapsulated in nickel plate. The nominal diameter of the silicon carbide abrasive grits was 0.025 inch. The tests were conducted at a rubbing speed of 1500 feet per second, an interaction rate of 2.7 mils per minute, and ambient temperature. Configuration B (Figure 1) was rubbed across the butt joint to simulate an engine rub across seal segment tile joints. A third specimen (Configuration **A**) was rubbed against the same type blade tip treatment at the same rubbing speed and interaction rate but at a seal temperature of ≈2800°F. The results of the ambient temperature rub tests (Table I) indicate that, with respect to volume wear factor (VWF), the structural ceramic turbine seal system is very inferior to the graded ZrO_2-NiCr seal system; an average VWF of 100 compared to 0.00001. Severe erosion and fracture of the seal specimen prevented obtaining VWF data during the hot rub test.

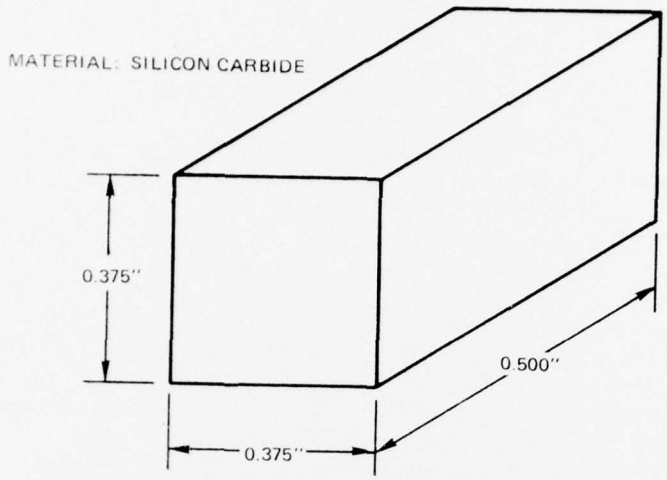

Figure 1 Structural Ceramic Erosion Specimen

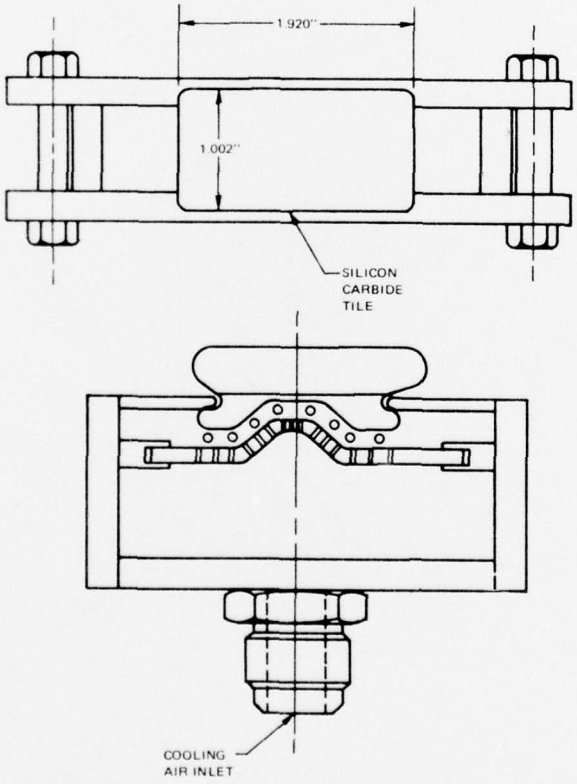

END VIEW, END PLATE REMOVED

Figure 3 Structural Ceramic Thermal Fatigue Specimen

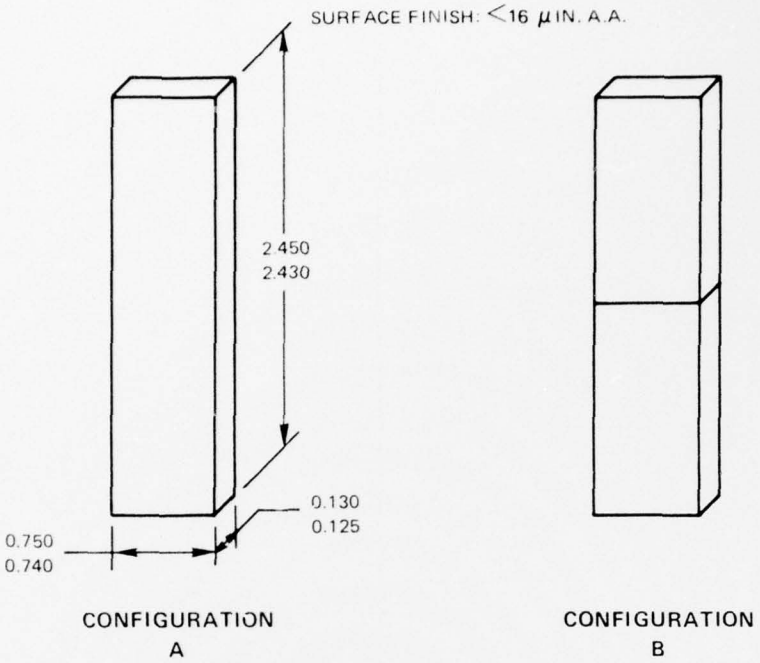

Figure 2 Revised Silicon Carbide Structural Ceramic Rub Test Specimen Design

TABLE I
SILICON CARBIDE STRUCTURAL CERAMIC SPECIMEN RUB TESTING

Sample	Rub Speed (ft/sec)	Blade Tip Temp.	Seal Temp (°F)	Interaction Rate (in/min)	Grit No.	Blade Tip Wear (in)	Seal Wear (in)	Average VWF
1	1500	Ambient	Ambient	0.0027	1	0.0074	0.0125×10^{-3}	
					2	0.00505	0.025×10^{-3}	
					3	0.0028	Negligible	80.0
2	1500	Ambient	Ambient	0.0027	1	0.014	0.050×10^{-3}	
					2	0.0152	Negligible	
					3	0.0158	0.050×10^{-3}	120.0
3	1500	–	2815	0.0027	1	b	d	
					2	b	d	
					3	c	d	

a. Volume Wear Factor (VWF) is equal to the blade tip wear volume divided by the seal wear volume
b. No apparent rub
c. Grit fractured off with 1/3 of plating matrix
d. Seal experienced fracture and severe erosion

STRUCTURAL CERAMIC TURBINE SEAL (Cont'd)

PRETEST MATERIAL CHARACTERIZATION

The hot pressed silicon carbide material was inspected for material density variations and inclusions, chemical composition, flexural strength, and microstructure.

High-sensitivity radiographic inspection of the as-received hot pressed silicon carbide billet (Norton Co. NC203) was performed. No inclusions or density variations were detected.

Spectrographic analysis of the as-received material (billet 437394) is shown in Table I. The table also includes a spectrographic analysis of silicon carbide billet 472-2* for comparison. Aluminum, boron, cobalt, and vanadium are present in significantly larger concentrations in the present billet than in the previously evaluated silicon carbide material. The possible effect of these impurities on mechanical properties is discussed below.

A photomicrograph of an etched, polished section from the center of billet 437394 is shown in Figure 1. This microstructure is typical of NC203 hot pressed silicon carbide.

Flexural strength evaluation was conducted on four specimens (1/8 x 1/8 x 2 inches) cut from the central region of the billet and diamond ground to final dimensions. The edges of the specimen face to be in tension were carefully rounded by hand with a water-cooled diamond grinding tool. The specimens were tested in four-point flexure with the minor span of 0.75 inch and the major span of 1.5 inches. The deflection rate was 0.020 inch per minute. At 2400°F the strength of two specimens was 32.8 and 26.2 ksi (29.5 ksi average). At ambient temperature strengths were 76.8 and 74.0 ksi (75.4 ksi average). These values are lower than the minimum values measured for other NC203 material at 2400°F and room temperature*. Since the material becomes disproportionately weaker with increasing temperature, it is likely that the increased amount of sintering aids (impurities) present is responsible. Increased concentrations of sintering aids are often associated with increased strain to failure, especially at high temperatures, and therefore may be a distinct advantage in brittle materials which are subjected to low average stresses.

*"Brittle Materials Design, High Temperature Gas Turbine", contract DAAG 46-71-C-0162, ARPA Order No. 1849, Agency Accession No. DAOD 4733.

TABLE I

CHEMICAL ANALYSIS OF SILICON CARBIDE BILLETS

WEIGHT PERCENT

	Billet 437394	Billet 472-2
Aluminum	1–10	1.0
Tungsten	0.5–5	3–5
Boron	0.05–0.5	0.002
Cobalt	0.05–0.5	– – –
Iron	0.05–0.5	0.1
Nickel	0.05–0.5	0.005
Vanadium	0.05–0.5	0.02
Chromium	0.01–0.1	0.01
Titanium	0.01–0.1	0.03
Copper	0.005–0.05	0.005
Zirconium	0.005–0.05	– – –
Magnesium	$<$0.01	0.001
Manganese	$<$0.01	0.001
Silicon & carbon	Balance	Balance

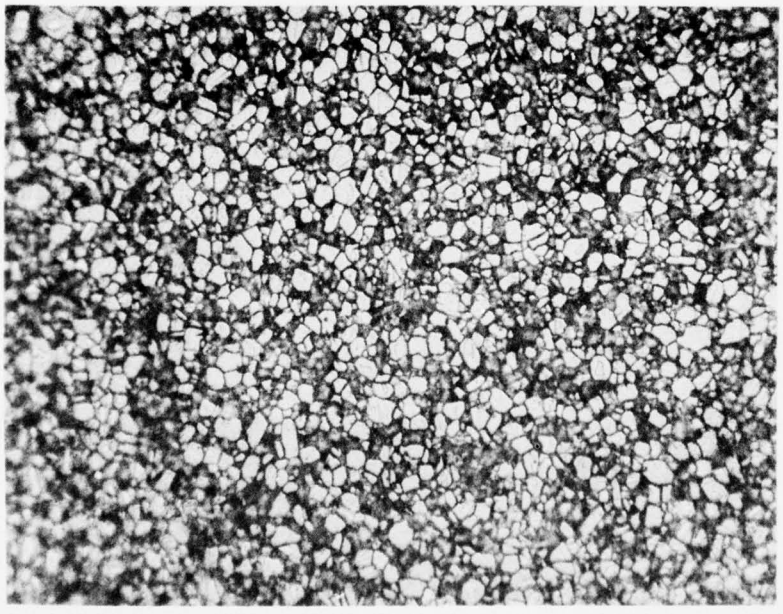

MAG: 500X

Figure 1 Microstructure of Silicon Carbide Billet 437394

FINAL DESIGN CERAMIC TURBINE SEAL

"Final" design incorporating the graded ZrO_2-NiCr system which allows very high surface temperatures, resulting in minimum cooling air required, also encompasses minimum leakage and rub tolerance with the most advanced state-of-the-art blade tip treatment to produce the most efficient high temperature turbine seal design.

The "final" advanced engine ceramic turbine seal design incorporates high temperature ZrO_2 on the entire gas path surface of the seals with mechanical concepts to minimize both the number of leakage points and the total leakage area. This will result in significant improvement in engine performance over previous all-metal seal designs.

The seal system (Figure 1) is made up of six 60° arc seal segments, each of which is fabricated by welding 3 component 20 degree arc segments together. The reduction from 32 segments minimizes the potential number of cooling air and gas path leaks. The remaining locations are sealed for radial and axial leakage using an improved version of the same concept incorporated in previous advanced engine turbine seals. The ZrO_2 surface material is abradable when used with abrasive tip treated blades allowing tighter blade tip clearances to be set for the engine.

The "final" advanced engine design was thermally analyzed using a two-dimensional finite-difference heat transfer computer program. All seal temperatures will remain within acceptable limits using $\approx 0.75\%$ W_{ae} cooling air distributed as shown in the flow map (Figure 2). The resulting thermal distribution is given in Figure 3 for the most severe thermal condition (full power hot spot) after a 20 mil rub interaction has occured.

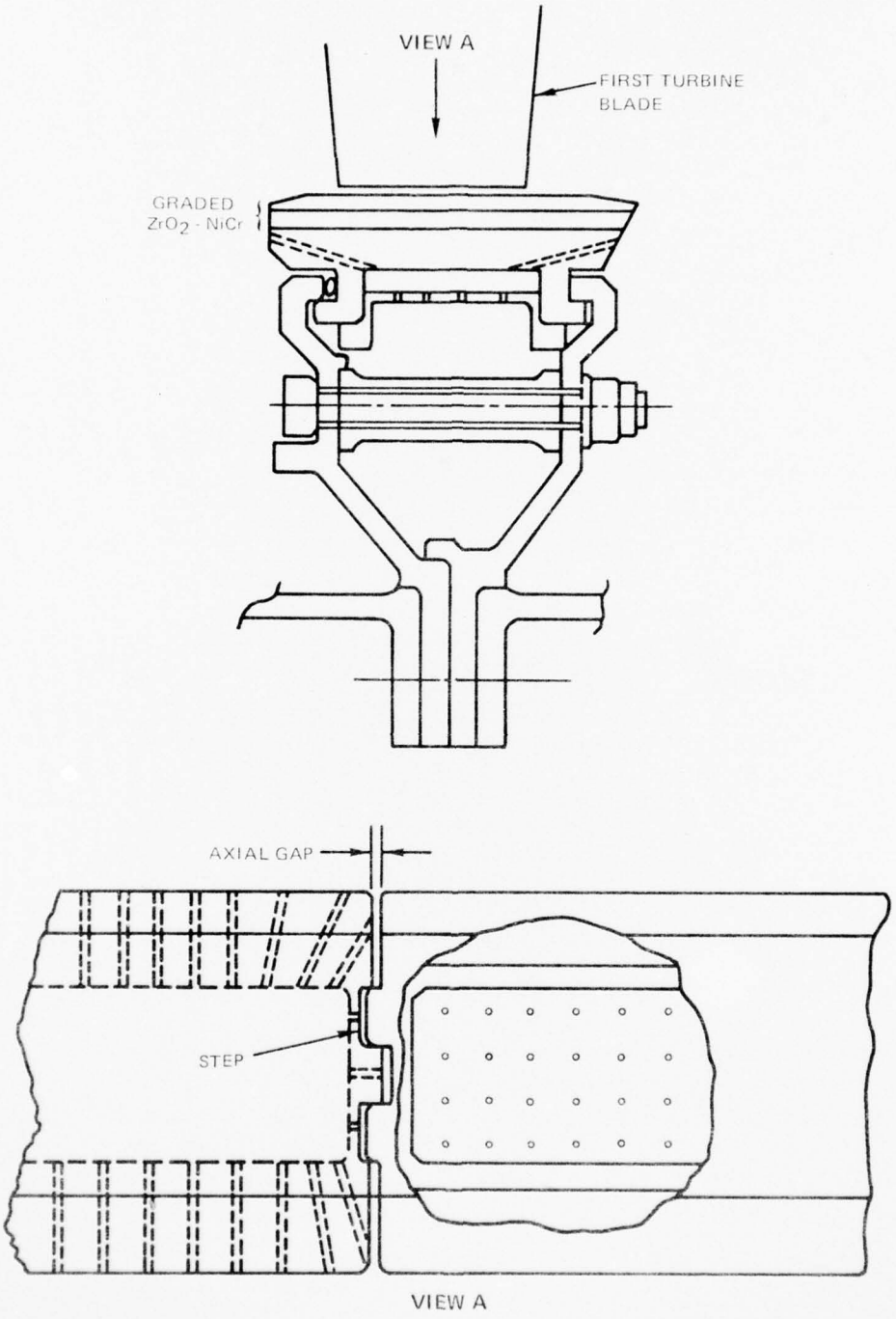

Figure 1 "Final" Advanced Engine Ceramic Turbine Seal Design

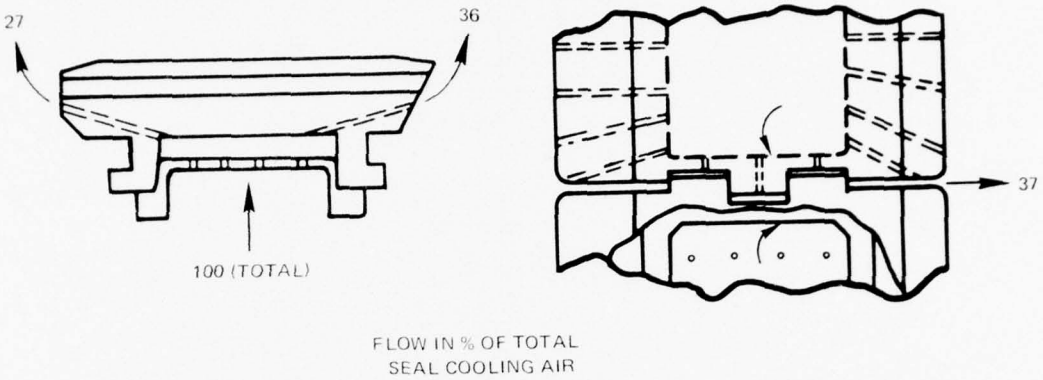

Figure 2 "Final" Advanced Engine Ceramic Seal Design Flow Map

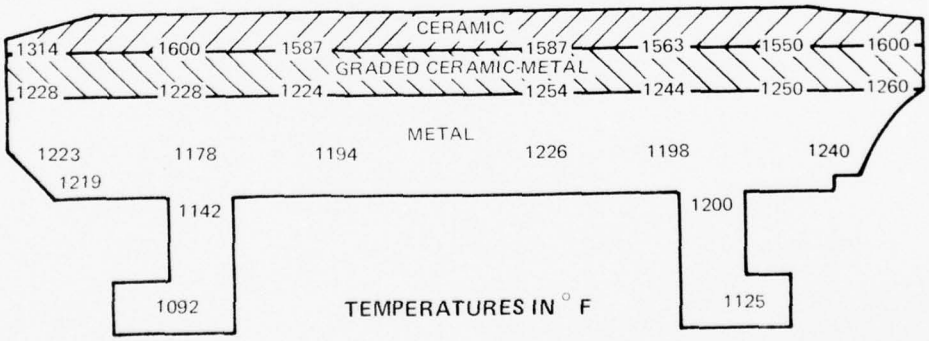

Figure 3 "Final" Advanced Engine Ceramic Seal Design Temperature Distribution at the Postrub Sea Level Takeoff Power Condition

FINAL DESIGN CERAMIC TURBINE SEAL (Cont'd)

Structural analysis was performed throughout an engine operating cycle using a two-dimensional finite element computer program, and accounting for three-dimensional effects with flat plate theory. A stress relief cycle was used to lower the stress free temperature to optimize the cyclic stresses within the allowable range of ceramic strength, which includes minimizing the magnitude of cyclic deflections. The maximum principal stresses are given in Table I. Invariably, these maximum principal stresses occur in the central portion of the seal relative to the edges and are below the experimental strengths in every case. Shear stresses at the seal edges are insignificant compared to the principal stresses.

Compressive plastic flow at power is expected to cause mud-flat carcking in the top 45 mils of the ZrO_2. This mud-flat cracking is stable and will not lead to system failure, and, because of the relatively high stiffness of the metal substrate, it will not lead to higher stresses in the ZrO_2 at any engine condition.

Structural analysis predicts that the corners of the seal will deflect radially outward approximately 0.013 inches relative to the center during the fabrication cycle. This distortion has been dimensionally accounted for during design. Table II shows the deflections predicted for the seal through the operating cycle relative to room temperature, and are considered minor.

TABLE I

ESTIMATED STRESS LEVELS FOR "FINAL" ADVANCED ENGINE CERAMIC SEAL (STRESS IN KSI)

Seal Layer	Room Temp.	30 Second Start Up	Idle	6 Second Accel.	Sea Level Take-off	12 Second Decel.
Ceramic	-5.4	-6.2	-0.3	-7.5	-5.1	-3.2
Intermediate	-2.3	-3.7	-3.8	-2.8	-4.5	-7.4
Metal	+15	+20	+14	+10	+7	+14

TABLE II

PREDICTED MAXIMUM OPERATING DEFLECTIONS* FOR "FINAL" ADVANCED ENGINE CERAMIC SEAL

	30 Second Warmup	Idle	6 Second Accel.	Sea Level Takeoff	12 Second Decel.
Deflection (mils)	1.0	–	2.8	−0.4	−3.6

*Relative to Room Temperature (Axial)